

Crystallography of homophase twisted bilayers: coincidence, union lattices and space groups

Denis Gratias* and Marianne Quiquandon

CNRS UMR 8247, Institut de Recherche de Chimie ParisTech, 11 rue Pierre et Marie Curie, 75005 Paris, France.

*Correspondence e-mail: denis.gratias@chimieparitech.psl.eu

Received 14 July 2022

Accepted 22 April 2023

Edited by M. L. A. N. De Las Peñas, Ateneo de Manila University, Philippines

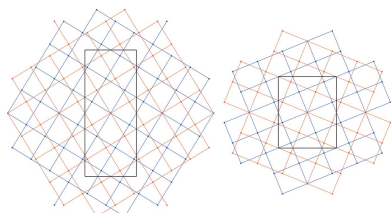
Keywords: bicrystallography with complex numbers; bilayers; coincidence lattices; space groups.

This paper presents the basic tools used to describe the global symmetry of so-called bilayer structures obtained when two differently oriented crystalline monoatomic layers of the same structure are superimposed and displaced with respect to each other. The 2D nature of the layers leads to the use of complex numbers that allows for simple explicit analytical expressions of the symmetry properties involved in standard bicrystallography [Gratias & Portier (1982). *J. Phys. Colloq.* **43**, C6-15–C6-24; Pond & Vlachavas (1983). *Proc. R. Soc. Lond. Ser. A*, **386**, 95–143]. The focus here is on the twist rotations such that the superimposition of the two layers generates a coincidence lattice. The set of such coincidence rotations plotted as a function of the lengths of their coincidence lattice unit-cell nodes exhibits remarkable arithmetic properties. The second part of the paper is devoted to determination of the space groups of the bilayers as a function of the rigid-body translation associated with the coincidence rotation. These general results are exemplified with a detailed study of graphene bilayers, showing that the possible symmetries of graphene bilayers with a coincidence lattice, whatever the rotation and the rigid-body translation, are distributed in only six distinct types of space groups. The appendix discusses some generalized cases of heterophase bilayers with coincidence lattices due to specific lattice constant ratios, and mechanical deformation by elongation and shear of a layer on top of an undeformed one.

1. Introduction

The discovery of strong electronic correlations and superconductivity in twisted bilayer graphene (Trambly de Laisardière *et al.*, 2010, 2012), with a so-called magic rotation angle close to 1.05° where the Fermi velocity vanishes, has significantly increased the interest in detailed study (Cao, Fatemi, Demir *et al.*, 2018; Cao, Fatemi, Fang *et al.*, 2018) of these kinds of low-dimension structures [see, for transition metal dichalcogenides, Naik & Jain (2018), Wu *et al.* (2019), Soriano & Lado (2020), Venkateswarlu *et al.* (2020)]. The eventual aim is to determine which symmetry property may explain the existence of flat bands in the electronic structure (Suarez Morell *et al.*, 2010): what, in the symmetry properties (if any) of twisted bilayers, is at the origin of this electronic localization?

A robust answer to this question requires a practical and simple crystallographic description of bilayer structures. This is the focus of the present work. The fundamental mathematical aspects of coincidence lattices at any dimensions are to be found in the very elaborated studies of Pleasants *et al.* (1996), Baake & Grimm (2006), Baake & Zeiner (2017). We focus here on the very elementary practical aspect of investigating the unique case of 2D bilayer structures.



OPEN ACCESS

Published under a CC BY 4.0 licence

Investigation of the symmetry properties of the superimposition of two 3D crystals, called bicrystals, was carried out in the 1980s (Gratias & Portier, 1982; Pond & Vlachavas, 1983) in the study of the properties of grain boundaries in metals and alloys. Although, at that time, these bicrystals were only theoretical concepts, their 2D versions of superimposing two monoatomic layers make sense in the present context as the idealization of a twisted bilayer considered as the superimposition of two infinitely thin monoatomic layers differently oriented by a twist rotation of angle α perpendicular to the layer plane and displaced with respect to each other by a translation τ in the plane.

The paper is organized as follows. Our first task is to enumerate which specific rotation angles α lead to a situation where two homophase layers share a common sublattice, say \mathcal{T}_α , of index Σ in Λ , and to explicitly give the expressions of these sublattices \mathcal{T}_α and those \mathcal{U}_α generated by the union of the lattices of the two layers. Our second task is to understand how these specific coincidence angles are distributed with respect to the values of the square length σ (identical to Σ for the square and hexagonal systems) of the coincidence unit-cell vectors. Our third task is to determine which space group \mathcal{N}_τ is generated for bilayers with coincidence lattices when the rigid-body translation τ varies at constant rotation α . Three appendices give the explicit illustration of the whole process in the case of twisted graphene bilayers and the conditions for coincidence and union lattices to exist in the case of heterophase bilayers obtained by dilatation and/or rotation or mechanical deformation.

We use the following notation: point groups are noted in capital letters like G or W ; space groups and translation groups are noted in calligraphic letters like \mathcal{G} or \mathcal{T}_α ; space symmetry operators (or functions in the complex plane as

discussed next) are noted as $\hat{\mathbf{a}}$ or $\hat{\mathbf{g}}$ whereas point symmetry operators are simply written as α or g .

2. Elementary bicrystallography

As already mentioned, homophase bilayers are ideally defined here as the superimposition of two identical monolayers on top of each other, forming an infinitely thin layer of matter. The twist operation, that transforms the monolayer I into II , is either a rotation–translation $\hat{\mathbf{a}}_\tau$ acting as $\hat{\mathbf{a}}_\tau r = (\alpha|\tau)r = \alpha r + \tau$, or a mirror translation (in all 2D enantiomorphic structures, these two descriptions are equivalent as they describe the same twist operation) $\hat{\mathbf{m}}_{\theta,\tau}$ oriented along a direction of angle θ with the x axis, acting as $\hat{\mathbf{m}}_{\theta,\tau} r = (m_\theta|\tau)r = m_\theta r + \tau$.

The original monolayer I has space group [we use the notations of Hahn (2005)] \mathcal{G} with point group Γ and lattice Λ showing the holohedral symmetry class of point group G_Λ with $G_\Lambda \geq \Gamma$ according to:

- (i) Oblique system $G_\Lambda = 2$: $\Gamma = 1, 2$;
- (ii) Rectangular system $G_\Lambda = 2mm$: $\Gamma = m, 2mm$;
- (iii) Square system $G_\Lambda = 4mm$: $\Gamma = 4, 4mm$;
- (iv) Hexagonal system $G_\Lambda = 6mm$: $\Gamma = 3, 3m, 6, 6mm$.

The corresponding group and lattice of the second monolayer II are given by

$$\mathcal{G}' = \hat{\mathbf{a}}_\tau \mathcal{G} \hat{\mathbf{a}}_\tau^{-1}, \quad \Gamma' = \alpha \Gamma \alpha^{-1} \text{ and } \Lambda' = \alpha \Lambda.$$

Since any point in the orbit of r under \mathcal{G} can be equivalently chosen, we characterize the transformation from layer I to II by the set $\hat{\mathbf{a}}_\tau \mathcal{G}$. The inverse transformation from II to I is given by $\mathcal{G} \hat{\mathbf{a}}_\tau^{-1} = \mathcal{G}(\alpha^{-1} | -\alpha^{-1}\tau)$ as shown in Fig. 1.

2.1. Using complex numbers for 2D crystallography

2D crystallography is particularly simple to handle using complex numbers. In fact, any 2D vector $V = (x, y)$ in an orthonormal reference frame of the plane is equivalently described by a complex number $z = x + iy \in \mathbb{C}$. Concerning the nodes of a 2D lattice $\Lambda(a, b)$ defined by its unit cell of vectors a and b , we choose the unit-cell vector a along the real axis and its length as the length unit with no loss of generality. The unit vector b is the complex number $b = \rho \exp(i\varphi)$ where ρ is the length of vector b in $|a|$ units and φ the angle of b with

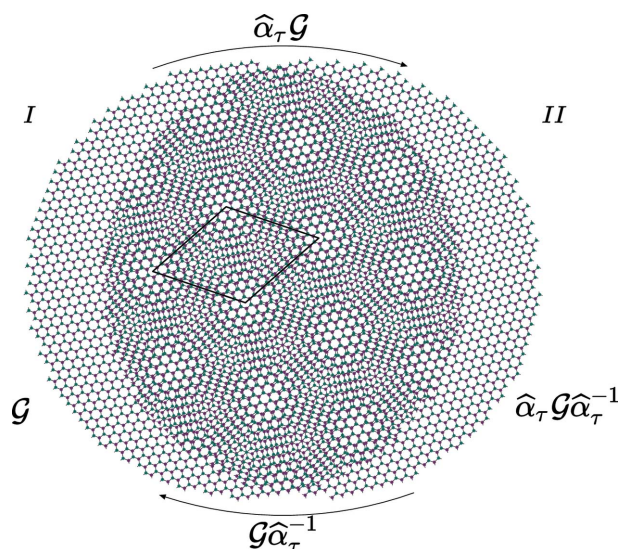


Figure 1
Passing from monolayer I to monolayer II is achieved by the set $\hat{\mathbf{a}}_\tau \mathcal{G}$ and from II to I by the inverse set $\mathcal{G} \hat{\mathbf{a}}_\tau^{-1}$. The overlap of the monolayers, designed here as a bilayer, generates its own symmetry that is a 2D space group if the two lattices Λ and Λ' have a common coincidence lattice $\mathcal{T} = \Lambda \cap \Lambda'$ and only a quasiperiodic symmetry otherwise.

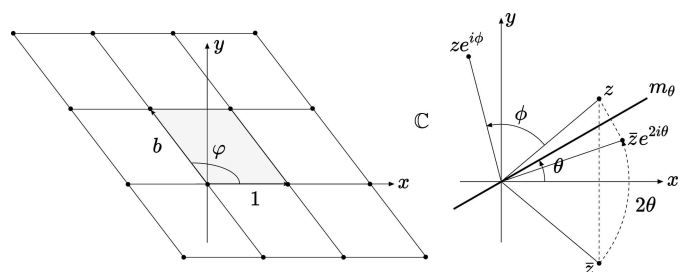


Figure 2
The lattice $\Lambda(a, b)$ with unit cell (a, b) is the set of complex numbers $z = n + m\rho \exp(i\varphi)$, $n, m \in \mathbb{Z}$, $\rho \in \mathbb{R}$, where the unit vector a is chosen as the unity along the real axis x and b is the complex number $b = \rho \exp(i\varphi)$. A rotation of angle ϕ around the origin transforms z into $z \exp(i\phi)$ and a mirror m_θ passing through the origin and oriented along the direction of angle θ transforms z into $\bar{z} \exp(2i\theta)$.

Table 1

2D lattices: the parameter a is the length unit ($a = 1$) along the real axis. All lattices are primitive except in the rectangular system with c -type lattices. Running indices n, m are integers. Here, $j = \exp(2i\pi/3)$.

System	Lattice $\Lambda(n, m)$	Unit cell ($a = 1$)	Angle (a, b)
Oblique	$[n + m\rho \exp(i\varphi)]$	$b = \rho$	φ
Rectangular	$(n + im\rho)$	$b = \rho$	$\pi/2$
	$(n + im\rho) \cup [n + \frac{1}{2} + i(m + \frac{1}{2})\rho]$	$b = \rho$	$\pi/2$
Square	$(n + im)$	$b = 1$	$\pi/2$
Hexagonal	$(n + jm)$	$b = 1$	$2\pi/3$

the real axis as shown in Fig. 2. A general primitive lattice Λ_p of unit vectors $a = 1$ and $b = \rho \exp(i\varphi)$ is then the set of complex numbers

$$\begin{aligned} \Lambda_p &= \{na + mb, n, m \in \mathbb{Z}\} \\ &= \{z = n + m\rho \exp(i\varphi), z \in \mathbb{C}, n, m \in \mathbb{Z}\}. \end{aligned}$$

[In addition, c -type lattices encountered in the rectangular symmetry class ($\varphi = \pi/2$) are defined as $\Lambda_c = \Lambda_p \cup \frac{1}{2}(1 + i\rho)\Lambda_p$.] The complex notations of the 2D lattices are given in Table 1.

The symmetry operations act as functions of complex variable $f(z)$ as elementary transformations of complex numbers:

- (i) A translation $u \in \mathbb{C}$ acts on a point z as $z \rightarrow u(z) = z + u$;
- (ii) A rotation ϕ around the origin transforms z into $z \rightarrow \phi(z) = z \exp(i\phi)$;
- (iii) A mirror m_θ passing through the origin and oriented in the direction θ transforms z into $z \rightarrow m_\theta(z) = \bar{z} \exp(2i\theta)$.

Space operators are the usual combinations of point symmetries and translations as shown in Table 2.

2.2. Coincidence angles for homophase bilayers

(This includes bilayers with different monolayers but sharing identical lattices.) General twisted bilayers are quasi-periodic structures built on a \mathbb{Z} module of rank 4. Specific cases arise for particular values of the rotation angle α , called coincidence angles, where the two initial lattices Λ and Λ' share a 2D sublattice \mathcal{T}_α , called the coincidence lattice characterized by the index Σ [defined by equation (9)], the ratio of the unit-cell sizes of \mathcal{T}_α and $\Lambda(\Lambda')$. This makes the nodes of the general \mathbb{Z} module of rank 4 condense on a 2D lattice \mathcal{U}_α called the union lattice, discussed later, in a similar way to generating periodic approximants from quasicrystals. In fact, as will be shown next, coincidence angles occur an infinite countable number of times and form a uniformly dense set of values on the real axis: any generic twisted bilayer is infinitely close to a coincidence situation which is the only case leading to exact space symmetries of the bilayer.

Finding the proper coincidence angles has been the subject of a very large number of publications for 2D and 3D crystals (see, for instance, Ranganathan, 1966; Grimmer, 1973, 1974, 1984). The most complete and recent analysis of coincidence

Table 2

2D symmetry operations ($g|t$) acting as functions $f(z)$ in the complex plane $z = x + iy$.

Symmetry operation	$f(z)$	$f^{-1}(z)$
Translation ($1 t$)	$z + t$	$z - t$
Inversion ($\bar{1} t$)	$-z + t$	$-z + t$
Rotation (ϕt)	$z \exp(i\phi) + t$	$(z - t) \exp(-i\phi)$
Mirror ($m_\theta t$)	$\bar{z} \exp(2i\theta) + t$	$(\bar{z} - \bar{t}) \exp(2i\theta)$

lattices in 2D crystals has been given by Romeu *et al.* (2012), a work that we reconsider here briefly using complex notations and that leads to a derivation which is simple and gives explicit expressions for the coincidence and union (homophase) lattices, as discussed next.

Let α be the rotation angle from the first monolayer to the second, both of point group G . The coincidence lattice, if any, is the common subset of the lattice translations of the monolayers:

$$\mathcal{T}_\alpha = \Lambda \cap \exp(i\alpha\Lambda).$$

A first necessary condition for a coincidence lattice to possibly exist is that a lattice row defined by the node (n, m) with $n, m \in \mathbb{Z}$, $\text{gcd}(n, m) = 1$ superimposes on another one (n', m') of the same orbit under \mathcal{G} by the rotation α around the origin:

$$\begin{aligned} (n', m') &\stackrel{\alpha}{\Rightarrow} (n, m) \text{ or } n + m\rho \exp(i\varphi) \\ &= \exp(i\alpha)[n' + m'\rho \exp(i\varphi)]. \end{aligned}$$

The possible generic solutions are listed below according to the crystalline system of the structure. {There are a few specific cases, in particular for the square system, with $n^2 + m^2 = n'^2 + m'^2$ where the nodes (n, m) and (n', m') do not belong to the same orbit under \mathcal{G} [for instance the nodes (3, 4) and (5, 0)]. These cases are not explicitly considered here.}

(i) Oblique system of point group 2: the generic orbit contains only two terms $(x, y), (\bar{x}, \bar{y})$, so that there are no solutions but the trivial rotation $\alpha = \pi$.

(ii) Rectangular system {this includes the special case of those specific oblique lattices where $2\rho \cos \phi = \pm 1$ which should be considered as c -type rectangular lattices $[cm(m)]$ } point group $2mm'$ ($\varphi = \pi/2$): the generic orbit contains four terms $(x, y), (\bar{x}, y), (x, \bar{y}), (\bar{x}, \bar{y})$; the two non-trivial solutions are those where (n', m') is deduced from (n, m) by the mirrors m_x ($n' = -n, m' = m$) and m'_y ($n' = n, m' = -m$).

(iii) Square system of point group $4mm'$ ($\varphi = \pi/2, \rho = 1$): in addition to the rectangle case, new solutions are $n' = \pm m, m' = \pm n$. All these solutions can be generated by using the mirror m_x and the mirror m'_{xy} rotated by $\pi/4$ up to additional $\pi/2$ rotations.

(iv) Hexagonal system $6mm'$ ($\varphi = 2\pi/3, \rho = 1$): here too, all possible solutions are obtained by using the mirror m_x and the mirror m' rotated from the x axis by $\pi/6$ up to additional rotations of $\pi/3$.

Hence, with the exception of the oblique system which presents no generic solutions, the rotation of a lattice node on top of one of its equivalents can be achieved using the two

mirror generators of these point groups (see, for instance, Coxeter, 1963) according to: rectangle ($2mm'$) mirrors in the directions $\theta = 0$ and $\pi/2$; square ($4mm'$) mirrors in the directions $\theta = 0$ and $\pi/4$; hexagonal ($6mm'$) mirrors in the directions $\theta = 0$ and $\pi/6$.

Let $\alpha = 2\delta$ be the rotation around the origin that superimposes the node $z' = \bar{z} \exp(2i\theta)$, on top of $z = n + m\rho \exp(i\varphi)$ related to z' by the mirror m_θ oriented along the direction θ as shown in Fig. 3. Putting $\sigma = z\bar{z}$, we note that $\sqrt{\sigma} \exp(i\theta) = z \exp(-i\delta)$ and therefore $\sqrt{\sigma} \exp(i\delta) = z \exp(-i\theta)$ so that

$$\sqrt{\sigma} \cos \delta = (n + m\rho \cos \varphi) \cos \theta + m\rho \sin \varphi \sin \theta \quad (1)$$

$$\sqrt{\sigma} \sin \delta = -(n + m\rho \cos \varphi) \sin \theta + m\rho \sin \varphi \cos \theta \quad (2)$$

and thus

$$\delta = \arctan \frac{-(n + m\rho \cos \varphi) \sin \theta + m\rho \sin \varphi \cos \theta}{(n + m\rho \cos \varphi) \cos \theta + m\rho \sin \varphi \sin \theta}. \quad (3)$$

These three relations apply for the rectangle, square and hexagonal systems with the following specific forms:

Rectangle ($\varphi = \pi/2, \theta = 0, \pi/2$):

$$\begin{cases} \sqrt{\sigma} \cos \delta_0 = n, \sqrt{\sigma} \sin \delta_0 = m\rho, \\ \delta_0 = \arctan \frac{m\rho}{n}, \\ \sqrt{\sigma} \cos \delta_{\pi/2} = m\rho, \sqrt{\sigma} \sin \delta_{\pi/2} = -n, \\ \delta_{\pi/2} = \arctan \frac{n}{m\rho} = \delta_0 - \pi/2. \end{cases} \quad (4)$$

Square ($\varphi = \pi/2, \rho = 1, \theta = 0, \pi/4$):

$$\begin{cases} \sqrt{\sigma} \cos \delta_0 = n, \sqrt{\sigma} \sin \delta_0 = m \\ \delta_0 = \arctan \frac{m}{n}, \\ \sqrt{\sigma} \cos \delta_{\pi/4} = \frac{1}{\sqrt{2}}(n + m), \sqrt{\sigma} \sin \delta_{\pi/4} = \frac{1}{\sqrt{2}}(m - n) \\ \delta_{\pi/4} = \arctan \frac{m-n}{n+m} = \delta_0 - \pi/4. \end{cases} \quad (5)$$

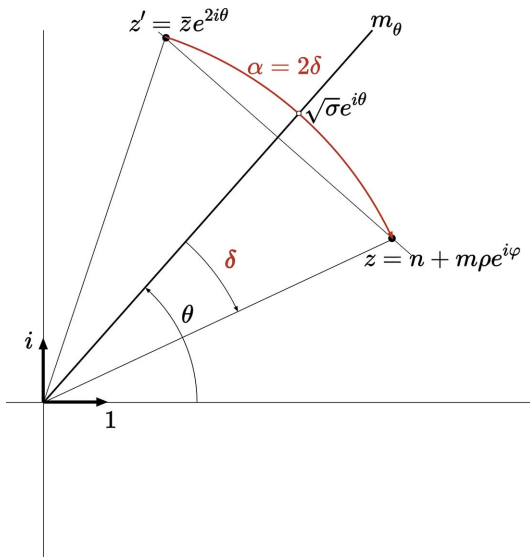


Figure 3

For all 2D systems except the oblique case, which has no generic solution, two homophase layers share the same crystallographic row defined by the lattice node $z = n + m\rho \exp(i\varphi)$, with n and m coprimes, if there exists an equivalent lattice node $z' = \bar{z} \exp(2i\theta)$ deduced from z by a mirror in the direction θ defined by: rectangle $\theta = 0, \pi/2$, square $\theta = 0, \pi/4$ and hexagonal $\theta = 0, \pi/6$.

Hexagonal ($\varphi = 2\pi/3, \rho = 1, \theta = 0, \pi/6$):

$$\begin{cases} 2\sqrt{\sigma} \cos \delta_0 = 2n - m, 2\sqrt{\sigma} \sin \delta_0 = m\sqrt{3}, \\ \delta_0 = \arctan \frac{m\sqrt{3}}{2n-m}, \\ 2\sqrt{\sigma} \cos \delta_{\pi/6} = n\sqrt{3}, 2\sqrt{\sigma} \sin \delta_{\pi/6} = 2m - n, \\ \delta_{\pi/6} = \arctan \frac{2m-n}{n\sqrt{3}} = \delta_0 - \pi/6. \end{cases} \quad (6)$$

These relations are necessary conditions for ensuring two equivalent lattice rows superimpose on each other by the rotation $\alpha = 2\delta$ and $\alpha = 2(\delta - \theta)$. Because these two solutions differ only by the constant rotation θ , we consider from now on the unique solution $\theta = 0$ defined by the basic relations

$$\sqrt{\sigma} \exp(i\delta) = n + m\rho \exp(i\varphi); \quad \delta = \arctan \frac{m\rho \sin \varphi}{n + m\rho \cos \varphi}, \quad (7)$$

remembering that with each solution δ ($0 \leq \delta \leq \theta$) is associated the solution δ' ($-\theta \leq \delta' = \delta - \theta \leq 0$).

2.2.1. Coincidence lattices in the rectangle system.

Ensuring one row in coincidence is of course not sufficient to generate a 2D coincidence lattice: this requires another non-collinear row of lattice nodes to be in coincidence for the same rotation angle.

We discard the oblique system that we know has no generic rows of coincidence whatever the rotation angle and thus no possible coincidence lattice. We focus now on the unique rectangle system since the square and hexagonal systems are specific high-symmetry cases of the rectangle one.

Let $\{T_1, T_2\}$ be the unit cell of the coincidence lattice \mathcal{T}_α we seek with $T_1 = n + im\rho$ in the rectangle system. Because \mathcal{T}_α , if it exists, shares at least the same symmetry class as the lattice of the monolayer (see, for instance, Gratias & Portier, 1982) – here the rectangular symmetry $2mm$ or higher – another coincidence vector $T_2 = n' + im'\rho$ exists that is aligned along $i\rho T_1$ up to a certain ratio r :

$$T_2 = ir\rho T_1 = -mr\rho^2 + irn\rho = n' + im'\rho, n', m' \in \mathbb{Z}, r \in \mathbb{Q}.$$

This requires $rn = m'$, thus $r \in \mathbb{Q}$ and $-mr\rho^2 = n'$ which is achieved if and only if $\rho^2 \in \mathbb{Q}$, i.e. $\rho^2 = p/q$, where p and q are coprime positive integers. Thus, σ is a rational number:

$$\sigma = n^2 + m^2 \rho^2 = \frac{qn^2 + pm^2}{q}$$

and $q\sigma = qn^2 + pm^2 \in \mathbb{Z}$ is a multiple of $\gamma = \text{gcd}(mp, nq)$.

These results confirm in a few calculation steps those obtained by Romeu *et al.* (2012) following a seminal paper by Ranganathan (1966) in the context of classical 3D crystallography. Here, coincidence lattices in homophase bilayers in the rectangular system exist if and only if the ratio $\rho = |b|/|a|$ is the square root of a rational number:

$$\rho = \sqrt{\frac{p}{q}}, p, q, \in \mathbb{N}.$$

[Oblique lattices with $2\rho \cos \varphi = 1$ as the hexagonal lattice can be considered as rectangular c -type lattices of parameters $(1, \rho' = \tan \varphi)$ and therefore show a 2D coincidence lattice when $\rho'^2 = \tan^2 \varphi = p/q$, with $p, q \in \mathbb{Z}$.] We conclude therefore that the coincidence angles for the rectangle system are

distributed as a uniformly dense countable set of points on the real axis as $\alpha = 2 \arctan \rho\eta$ with $\eta \in \mathbb{Q}$.

2.2.2. Explicit expression of the coincidence lattice in the rectangle system. The unit vector T_2 of \mathcal{T}_α is the smallest vector along $i\rho T_1$ with integer coordinates

$$T_2 \propto i\rho T_1 = (-m\rho^2 + in\rho) = \frac{1}{q}(-mp + inq\rho).$$

It is obtained by multiplying $i\rho T_1$ by q and then dividing the result by $\gamma = \text{gcd}(mp, nq)$:

$$T_2 = \frac{1}{\gamma}(-mp + inq\rho) = \frac{q}{\gamma}(-m\rho^2 + in\rho) = i\frac{q}{\gamma}\rho T_1.$$

We first note that putting $nq = r\gamma$ and $mp = s\gamma$ with $r, s \in \mathbb{Z}$, we obtain $T_2 = -s + ir\rho$, which explicitly shows that, indeed, T_2 belongs to Λ . We then observe that, as required, T_2 is orthogonal to T_1 , but the length of T_2 is in the ratio ρ with the length of T_1 only when $q = \gamma$ and therefore, although with at least the same symmetry class as Λ , the coincidence lattice is not necessarily homothetic to Λ in the general case as illustrated in Fig. 4.

Because of relations (7), we have

$$\begin{aligned} T_1 &= n + im\rho = \exp(i\delta)\sqrt{\sigma} \text{ and} \\ T_2 &= i\frac{q}{\gamma}\rho T_1 = i\exp(i\delta)\sqrt{\sigma}\frac{q}{\gamma}\rho, \end{aligned}$$

so that the coincidence lattice \mathcal{T}_α is explicitly given by

$$T_\alpha = NT_1 + MT_2 = \exp(i\delta)\sqrt{\sigma}\left(N + iM\frac{q}{\gamma}\rho\right), \quad N, M, \in \mathbb{Z}, \quad (8)$$

showing that the coincidence lattice \mathcal{T}_α is generated by a lattice characterized by $a' = 1$ and $b' = i(q/\gamma)\rho$, rotated by δ with respect to Λ and linearly dilated by $\sqrt{\sigma}$.

Since Σ is the index of the translation group \mathcal{T}_α in Λ , i.e. the ratio of the surfaces of the unit cell of the coincidence lattice \mathcal{T}_α with respect to the one of the lattice Λ , we find

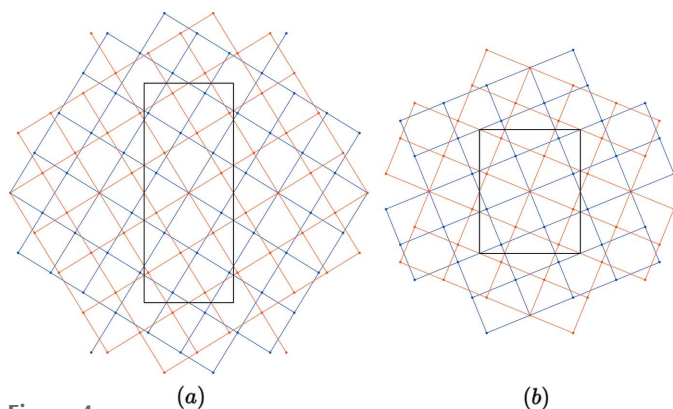


Figure 4
Example of coincidence lattices in black in the rectangular system $\rho = \sqrt{3}/2$ ($p = 3, q = 2$) for: (a) $n = 2, m = 1, \gamma = 1, T_1 = (2, 1), T_2 = (-3, 4), |T_2| = 2\rho|T_1|, \sigma = (11/2), \Sigma = 11, \delta = 31.482^\circ$; (b) $n = 1, m = 2, \gamma = 2, T_1 = (1, 2), T_2 = (-3, 1), |T_2| = \rho|T_1|, \sigma = \Sigma = 7, \delta = 67.792^\circ$.

$$\Sigma = \frac{|T_1| |T_2|}{\rho} = \frac{q\sigma}{\gamma} = \frac{1}{\gamma}(n^2q + m^2p) \in \mathbb{N}^+ \quad (9)$$

which is, indeed, an integer since $\gamma = \text{gcd}(mp, nq)$ is a divisor of $n^2q + m^2p$.

2.2.3. The union lattice. The other fundamental translation group is the group \mathcal{U}_α generated by the union of the lattice translation groups of the two crystals:

$$\begin{aligned} \mathcal{U}_\alpha &= \Lambda \cup \exp(i\alpha)\Lambda = \{h + h' \exp(i\alpha) + i\rho[k + k' \exp(i\alpha)]; \\ &h, k, h', k' \in \mathbb{Z}\} \end{aligned}$$

or

$$\begin{aligned} \mathcal{U}_\alpha &= \exp(i\delta)\{h \exp(-i\delta) + h' \exp(i\delta) \\ &+ i\rho[k \exp(-i\delta) + k' \exp(i\delta)]\} \\ &= \frac{\exp(i\delta)}{\sqrt{\sigma}}[nH + m\rho^2K' + i\rho(mH' + nK)] \\ &= \frac{\exp(i\delta)}{q\sqrt{\sigma}}[nqH + mpK' + iq\rho(mH' + nK)], \end{aligned}$$

where $H = h + h', H' = h' - h, K = k + k', K' = k - k', N, M \in \mathbb{Z}$.

Therefore

$$\mathcal{U}_\alpha = \frac{\gamma \exp(i\delta)}{q\sqrt{\sigma}}\left(N + iM\frac{q}{\gamma}\rho\right) = \frac{\gamma}{q\sigma}T_\alpha = \frac{1}{\Sigma}T_\alpha. \quad (10)$$

This shows that, for any coincidence angle and any symmetry class larger than or equal to the rectangular one, \mathcal{U}_α is homothetic to \mathcal{T}_α in the linear ratio $1/\Sigma$ (this ratio applies on each unit vector leading thus to a relative density of nodes $\text{card } \mathcal{U}_\alpha/\mathcal{T}_\alpha = \Sigma^2$). It is easily demonstrated that this relation holds for the square and hexagonal (see Appendix A) systems with the coincidence lattices given by

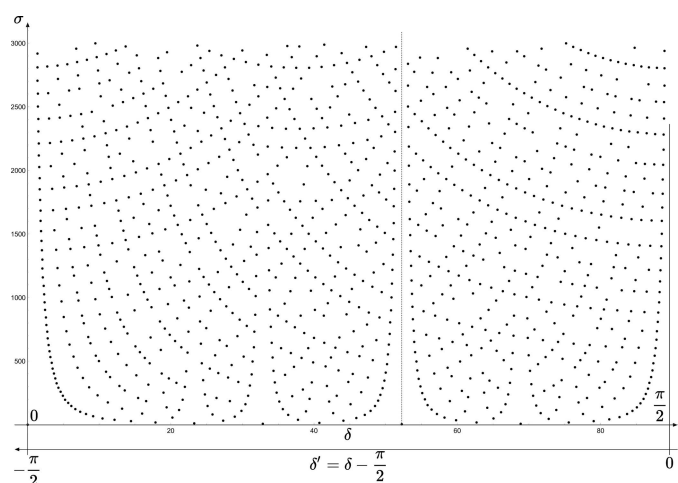


Figure 5
We visualize the set of coincidence angles in plotting the values of the coincidence angles $0 \leq \delta = \alpha/2 = \arctan mp/n \leq \theta$ as a function of the coincidence length $\sigma = n^2 + m^2\rho^2$ of the generating coincidence node (n, m) . Here, the example of the rectangle system with $\rho = \sqrt{5}/3$ for $0 \leq \delta \leq \pi/2$; the other solution $\delta' = \delta - \pi/2$ is obtained on the same diagram by exploring the x axis from $-\pi/2$ to 0. The vertical dashed line corresponds to $n = m = 1$, i.e. $\delta = \arctan \rho$.

$$\begin{aligned} \text{Square } \mathcal{T}_\alpha &= \sqrt{\sigma} \exp(i\delta)(N + iM), \\ \text{Hexagonal } \mathcal{T}_\alpha &= \sqrt{\sigma} \exp(i\delta)(N + jM). \end{aligned} \quad (11)$$

2.3. Coincidence patterns $\mathcal{P} = (\delta, \sigma)$

A classical scheme in metallurgy consists of collecting all the possible coincidence angles α , each associated with its Σ index, in a general pattern \mathcal{P} of points (α, Σ) which is the superimposition of all the coincidence angles equivalent to α with respect to the intrinsic symmetries of the layer, each associated with its Σ . In the case of a rectangle system, this pattern can exhibit quite a complicated fine structure due to the arithmetic irregularities introduced by the term q/γ in the definition of Σ seen in equation (9). Moreover, this kind of pattern is heavily redundant because of the superimposition of several rotations that are equivalent with respect to the inner symmetry of the layer. In fact, as shown in Fig. 5, a simpler and equally informative pattern is obtained by plotting only one rotation representative in the elementary sector of the point group of the monolayer, as a function of the square length of the superposition node (n, m) instead of Σ :

$$\begin{aligned} \mathcal{P}(n, m) &= \left(0 \leq \alpha/2 = \delta = \arctan \frac{m\rho \sin \varphi}{n + m\rho \cos \varphi} \leq \theta, \right. \\ &\quad \left. \sigma = n^2 + m^2 \rho^2 + 2nm\rho \cos \varphi \right). \end{aligned}$$

A very basic fact is that since the coincidence angles are defined by lattice vectors (n, m) , where n and m are coprime

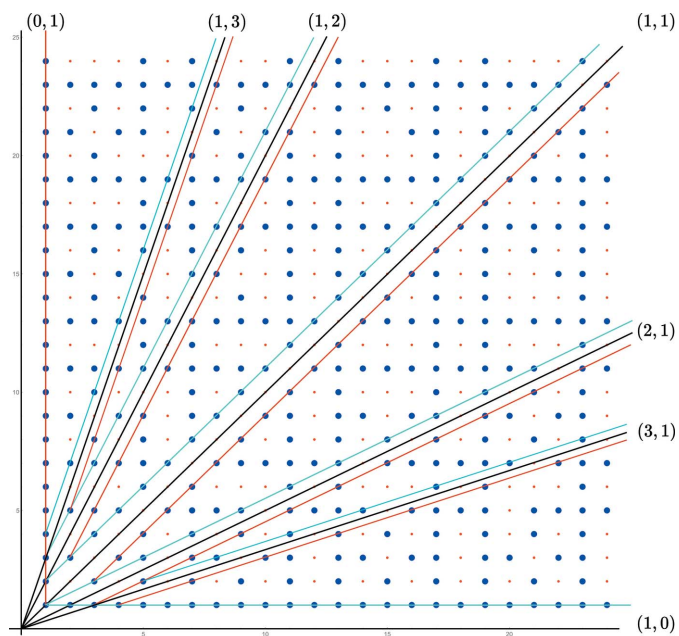


Figure 6
The points of coincidence are defined by coprime pairs of integers (n, m) , i.e. by fractions m/n in their irreducible forms. Plotted on the nodes of a lattice, they generate the so-called set \mathcal{V} of points visible from the origin made of the lattice points drawn in blue. Each rational row of this set, as those drawn in colors, is associated with a branch of points with the same colors in the coincidence pattern of Fig. 7.

integers, these vectors point to those nodes of a 2D lattice known as the set of points visible from the origin, noted here \mathcal{V} , as shown in Fig. 6. All points (δ, σ) of the coincidence pattern \mathcal{P} are in a one-to-one correspondence with those (n, m) , of \mathcal{V} .

In particular, rational rows in the set \mathcal{V} faithfully mirror the branches in \mathcal{P} that are asymptotically converging to specific angles δ characterized by their coincidence nodes (n, m) with $\tan(\delta) = \rho m/n$ as exemplified by the rows and corresponding branches drawn in cyan and purple in Figs. 6 and 7.

The simplest way to classify and order these branches is to label them according to Farey sequences $f(N)$ (see, for instance, Hardy & Wright, 1979). The Farey sequence of order N , noted $f(N)$, is the set of fractions m/n where m and n are coprime integers, associated with the nodes (n, m) of the set \mathcal{V} [see, for instance, in a different context Philippon (2008)], and such that $0 < m < n \leq N$, ordered by size.

We note the following properties:

(i) For any two elements of a sequence, corresponding in the set \mathcal{V} to the nodes (n_0, m_0) pointing in the direction $\tan(m_0/n_0)$ and (n_1, m_1) pointing in the direction $\tan(m_1/n_1)$, with $m_0/n_0 < m_1/n_1$, the vector $(n_0 + n_1, m_0 + m_1)$ pointing along their diagonal is such that

$$\frac{m_0}{n_0} < \frac{(m_0 + m_1)}{(n_0 + n_1)} < \frac{m_1}{n_1},$$

with $(n_0 + n_1)m_1 - (m_0 + m_1)n_1 = n_0(m_0 + m_1) - m_0(n_0 + n_1) = n_0m_1 - m_0n_1$.

(ii) If two elements i and j are consecutive ($j = i + 1$) in a sequence with $m_i/n_i < m_j/n_j$ then $n_i m_j - m_i n_j = 1$. Because of Bezout's identity, we deduce that beyond (n_i, m_i) and (n_j, m_j) being coprimes, the pairs (n_i, n_j) and (m_i, m_j) are also coprimes.

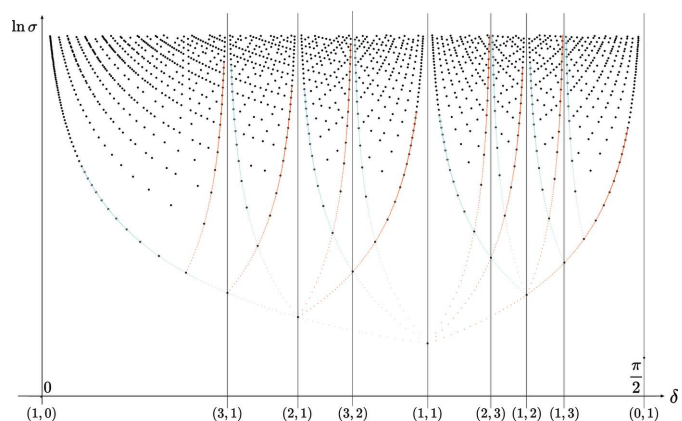


Figure 7
Distribution of the coincidence angles $\tan(\delta) = \rho m/n$, $n, m > 0$ versus $\sigma = n^2 + m^2 \rho^2$ in logarithmic scale, for the rectangle lattice with $\rho = \sqrt{3}/2$. The points are distributed on branches asymptotically converging to specific coincidence angles $\delta = \arctan(\rho m_i/n_i)$ where the points (n_i, m_i) belong to (extended) Farey sequences generated from the initial pair $[(1, 0), (0, 1)]$; here, the optimum branches generated by the Farey sequence $F_r(3)$ asymptotic by lower (purple) and upper (cyan) values are underlined with the same colors as their corresponding rows on the set \mathcal{V} of Fig. 6.

In fact, because the coincidence angles α run between 0 and π for the rectangle system, the sequences we are interested in here are extended Farey sequences (Halphn, 1877), noted $F_r(N)$, made of the standard Farey sequence $f(N)$ between (1, 0) and (1, 1) completed by the sequence from (1, 1) to (0, 1), obtained in adding to the original sequence the inverse fractions n/m in opposite order. Such typical extended sequences for the rectangular system, where $0 \leq \delta \leq \pi/2$, are

$$\begin{aligned} F_r(0) &= [(1, 0), (0, 1)] \\ F_r(1) &= [(1, 0), (1, 1), (0, 1)] \\ F_r(2) &= [(1, 0), (2, 1), (1, 1), (1, 2), (0, 1)] \\ F_r(3) &= [(1, 0), (3, 1), (2, 1), (3, 2), (1, 1), (2, 3), \\ &\quad (1, 2), (1, 3), (0, 1)] \end{aligned}$$

etc.

For the square system, the possible twist angles run from 0 to $\pi/2$ with the basic sequences ($0 \leq \delta \leq \pi/4$)

$$\begin{aligned} F_s(1) &= [(1, 0), (1, 1)] \\ F_s(2) &= [(1, 0), (2, 1), (1, 1)] \\ F_s(3) &= [(1, 0), (3, 1), (2, 1), (3, 2), (1, 1)] \\ F_s(4) &= [(1, 0), (4, 1), (3, 1), (2, 1), (3, 2), (4, 3), (1, 1)] \end{aligned}$$

etc.

For the hexagonal system, with twist angles extending from 0 to $\pi/3$, the sequences ($0 \leq \delta \leq \pi/6$) are

$$\begin{aligned} F_h(2) &= [(1, 0), (2, 1)] \\ F_h(3) &= [(1, 0), (3, 1), (2, 1)] \\ F_h(4) &= [(1, 0), (4, 1), (3, 1), (2, 1)] \\ F_h(5) &= [(1, 0), (5, 1), (4, 1), (3, 1), (5, 2), (2, 1)] \end{aligned} \quad (12)$$

etc.

2.4. Invariance property of the branches

Defining branches of points in the coincidence pattern is pertinent when the points of the same branch, described by a running index k , share the same property independent of this index. To determine which invariance property a branch corresponds to, we note that, because of relations (1), (2) and (3), any two points (δ, σ) , associated with the coincidence node (n, m) , and (δ', σ') , associated with (n', m') , of the same coincidence pattern are related by

$$\sqrt{\sigma\sigma'} \sin \Delta_{\delta,\delta'} = \rho \sin \varphi(n'm - m'n), \quad (13)$$

where $\Delta_{\delta,\delta'} = \delta - \delta'$.

Relation (13) is the key for characterizing the invariance rule for each branch of the pattern.

We consider the case of the rectangle system ($\varphi = \pi/2$) and choose two Farey neighbor terms (n_0, m_0) and (n_1, m_1) such that $n_0m_1 - m_0n_1 = 1$ and $m_0/n_0 < m_1/n_1$. We put $\sigma_0 = n_0^2 + \rho^2m_0^2$, $\sigma_1 = n_1^2 + \rho^2m_1^2$, $\tan \delta_0 = \rho m_0/n_0$ and $\tan \delta_1 = \rho m_1/n_1$.

We consider the set of nodes

$$n_{k,k'} = kn_0 + k'n_1, m_{k,k'} = km_0 + k'm_1, k, k' \in \mathbb{Z} \quad (14)$$

under their irreducible form [$\text{gcd}(n_{k,k'}, m_{k,k'}) = 1$], defining the points in \mathcal{P} :

$$\begin{cases} \delta_{k,k'} &= \arctan \rho \frac{(km_0 + k'm_1)}{kn_0 + k'n_1}, \\ \sigma_{k,k'} &= k^2\sigma_0 + k'^2\sigma_1 + 2kk'\beta \end{cases} \quad (15)$$

with $\beta = (n_0n_1 + \rho^2m_0m_1)$.

As shown in Fig. 6, at constant k' and running k , these nodes $(n_{k,k'}, m_{k,k'})$ describe rows in \mathcal{V} that are parallel to the direction (n_0, m_0) . At constant k and running k' , they describe rows in the direction (n_1, m_1) . These two rows intersect at the node $(n_0 + n_1, m_0 + m_1)$.

Observing that

$$\begin{aligned} n_0m_{k,k'} - m_0n_{k,k'} &= n_0(km_0 + k'm_1) - m_0(kn_0 + k'n_1) \\ &= k'(n_0m_1 - m_0n_1) = k', \forall k \in \mathbb{Z} \end{aligned} \quad (16)$$

$$\begin{aligned} m_1n_{k,k'} - n_1m_{k,k'} &= m_1(kn_0 + k'n_1) - n_1(km_0 + k'm_1) \\ &= k(m_1n_0 - n_1m_0) = k, \forall k' \in \mathbb{Z}, \end{aligned} \quad (17)$$

we note that at constant k' and running k , the points $(n_{k,k'}, m_{k,k'})$ describe a set of branches in \mathcal{P} , one for each value of k' , asymptotic (by upper values for $k' > 0$ and by lower values for $k' < 0$) to δ_0 for $k \rightarrow \infty$ where all points share the invariance property:

$$\forall k \in \mathbb{Z}, \sqrt{\sigma_{k,k'}\sigma_0} \sin \Delta_{(k,k'),0} = \rho k'. \quad (18)$$

Similarly, from relation (17), at constant k and running k' , corresponds a set of branches asymptotic (by upper values for $k > 0$ and by lower values for $k < 0$) to δ_1 for $k' \rightarrow \infty$ sharing the invariance property

$$\forall k' \in \mathbb{Z}, \sqrt{\sigma_1\sigma_{k,k'}} \sin \Delta_{1,(k,k')} = \rho k. \quad (19)$$

Concerning the irreducibility property, we note that $n_{k,k'}$ and $m_{k,k'}$ are both multiples of $\text{gcd}(k, k')$ and therefore k and k' must be coprime for the node $(n_{k,k'}, m_{k,k'})$ to belong to \mathcal{V} . Thus, any row in the set generated by a running $k(k')$ at constant $k'(k)$ exhibits only the points that are not multiples of the prime factors of the constant $k'(k)$. For example, in the Farey sequence $F(0) = [(1, 0), (0, 1)]$ where $(n_{k,k'}, m_{k,k'}) = (k, k')$, the rows parallel to the x corresponding to running k at constant k' show, in increasing k' order: all k values for $k' = 1$, only odd values of k for $k' = 2$, k not a multiple of 3 for $k' = 3$, k not a multiple of 2 and 3 for $k' = 6$ etc. The densest rows correspond to k' being a prime number. The same behavior is to be found for the rows parallel to the y direction and, extraordinarily enough, for any row parallel to a rational direction.

The $k(k')$ branches associated with the smallest values of $\sigma_{k,k'}$, designated here as optimal branches because they generate the smallest coincidence unit cell, are those where the constant $k(k')$ in relations (16) and (17) is the unity. These are the branches and associated rows colored, respectively, in cyan and purple in Figs. 6 and 7.

The two optimal branches in k and k' defined by the neighbor nodes (n_0, m_0) , (n_1, m_1) in the Farey sequence intersect at the node defined by $k = k' = 1$, i.e. at the node $(n_0 + n_1, m_0 + m_1)$ which is precisely the term inserted

between the two original nodes in the Farey sequence next to the original one.

2.5. Analytical expression of the optimal branches

Although the coincidence angles form a dense enumerable set of points on the trigonometric circle, the proximity of two alpha values does not ensure that of their corresponding σ values. This happens only when the two angles are on the same branch. Two branches are particularly important which are asymptotic to the angles of the generating mirrors of the point symmetry of the lattice of the monolayer, i.e. $\theta = 0$ for all systems, with additional $\theta = \pi/2$ for a rectangle, $\theta = \pi/4$ for a square and $\theta = \pi/6$ for a hexagonal system. They have a particular importance for bilayers with very small rotations as they allow us to choose the smallest-sized coincidence lattices closest to the angle we seek generating the smallest atomic model to be used in electronic calculations.

In the rectangle system, the two extreme asymptotic angles are $\theta = 0$ and $\pi/2$ associated with the two extreme branches defined by the Farey sequence $[(n_0, m_0) = (1, 0), (n_1, m_1) = (0, 1)]$. The relation (4) leads to

$$\sigma_0 = 1, \sigma_1 = \rho^2, \beta = 0$$

$$\theta = 0 \left\{ \begin{array}{l} n_{k,1} = k, m_{k,1} = 1, \sigma_{k,1} = k^2 + \rho^2 \\ \sin \delta_{k,1} = \frac{\rho}{\sqrt{k^2 + \rho^2}} \end{array} \right.$$

$$\theta = \pi/2 \left\{ \begin{array}{l} n_{1,k'} = 1, m_{1,k'} = k', \sigma_{1,k'} = 1 + k'^2 \rho^2 \\ \sin \delta_{1,k'} = \frac{1}{\sqrt{k'^2 \rho^2 + 1}} \end{array} \right.$$

We assume $\rho > 1$ ($p > q$). Using $\rho^2 = p/q$ with $\Sigma = q\sigma/\gamma$ and $\gamma = \text{gcd}(mp, nq)$, we find

$$\Sigma_{k,1} = \frac{q}{\text{gcd}(p, k)} \sigma_{k,1}, \Sigma_{1,k'} = \frac{q}{\text{gcd}(q, k')} \sigma_{1,k'}$$

We first observe, as shown in Fig. 8, that each time k and p share the same divisor, $\Sigma_{k,1}$ changes its value so that the initially unique $\sigma_{k,1}$ branch splits into ν subbranches $\Sigma_{k,1}^\nu$, where ν is the number of divisors of p . [Let $n = a^{p_1} \times b^{p_2} \times c^{p_3} \times \dots$ be the positive integer of prime factors a, b, c, \dots ; the number of its divisors is $(p_1 + 1) \times (p_2 + 1) \times (p_3 + 1) \times \dots$] Similarly, $\sigma_{1,k'}$ splits into μ subbranches $\Sigma_{1,k'}^\mu$, where μ is the number of divisors of q .

We then note that the same angle δ is shared by the two branches at steps, respectively, k and k' when $kq = pk'$, i.e. for $k = p\ell, k' = 1$ for one branch and $k' = q\ell, k = 1$, for the other, $\ell \in \mathbb{Z}$. At that stage $q\sigma_{p\ell,1} = p\sigma_{1,q\ell}$ and therefore $\Sigma_{p\ell,1} = (q/p)\sigma_{p\ell,1} = \sigma_{1,q\ell} = \Sigma_{1,q\ell}$. The two branches superimpose every p steps for one branch and q steps for the other with the same Σ values. Hence, the optimal branch for small angles in the rectangle system ($\rho^2 = p/q, p > q$) is found to be

$$n = 1, m = q\ell, \ell \in \mathbb{N}, \alpha_\ell = 2 \arctan \rho q\ell, \sigma_\ell = pq\ell^2 + 1$$

$$\sin \delta_\ell = \frac{1}{\sqrt{\sigma_\ell}} \text{ with } \delta_\ell = \frac{\pi}{2} - \delta_\ell \tag{20}$$

with a primitive lattice of parameters $A = 1 + i\rho q\ell, B = -p\ell + i\rho$ that condenses to a c -type lattice $(A + B)/2, (A - B)/2$ when p, q and ℓ are all three simultaneously odd.

For the square system, the situation is much simpler since here $\sigma = \Sigma$. The Farey sequence to be used here is $[(1, 0), (1, 1)]$ out of which we obtain

$$\sigma_0 = 1, \sigma_1 = 2, \beta = 1$$

$$\theta = 0 \left\{ \begin{array}{l} n_{k,1} = 1 + k, m_{k,1} = 1, \sigma_{k,1} = k^2 + 2k + 2 \\ \sin \delta_{k,1} = \frac{1}{\sqrt{k^2 + 2k + 2}} \end{array} \right.$$

$$\theta = \pi/4 \left\{ \begin{array}{l} n_{1,k'} = 1 + k', m_{1,k'} = k', \sigma_{1,k'} = 2k'^2 + 2k' + 1 \\ \sin \delta_{1,k'} = \frac{1}{\sqrt{4k'^2 + 4k' + 2}} \end{array} \right.$$

The same angle δ is shared by the two branches each time $k = 2k'$ with, then, $\sigma_{k,1} = 2\sigma_{1,k'}$. This is easily understood by noting that $k = 2k'$ implies $n_{k,1} + m_{k,1} = 2 + 2k'$ and $n_{k,1} - m_{k,1} = 2k'$ both even, which lead directly to $n_{1,k'} = 1 + k', m_{1,k'} = k'$ with a σ value twice smaller. The branch

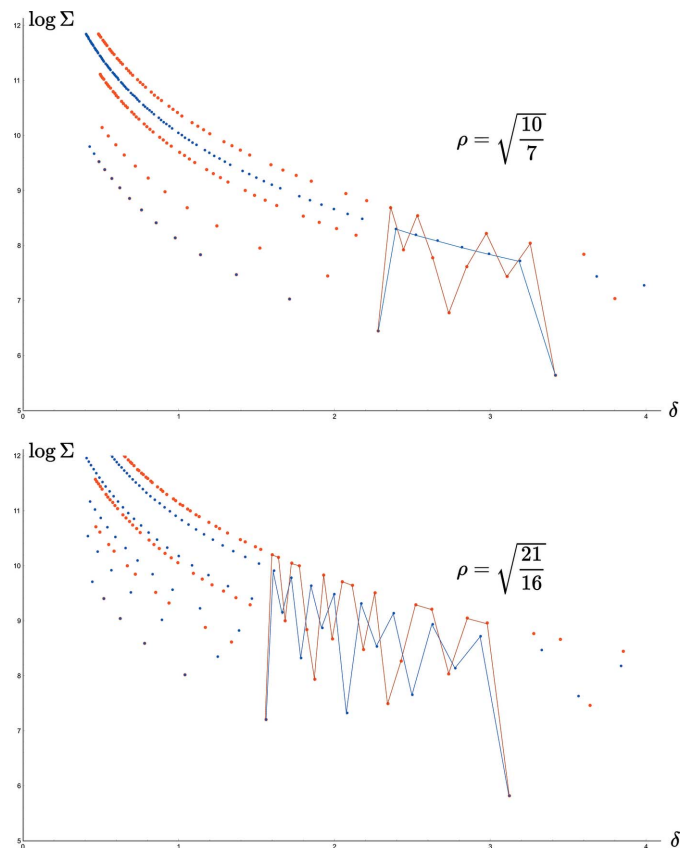


Figure 8 Splitting of the optimal branches as plotted against Σ instead of σ in the rectangle system for the cases $\rho = \sqrt{10/7}$ and $\rho = \sqrt{21/16}$. The red dots and lines correspond to $\Sigma_{k,1}$ and the blue dots and lines to $\Sigma_{1,k'}$. In the first case, $p = 2 \times 5$ the red branch splits into four subbranches in the ratio 1, 2, 5 and 10, and since $q = 7$, the blue branch splits into two subbranches of ratio 1 and 7. In the second case, $p = 21 = 3 \times 7$, the red branch splits into four subbranches in the ratio 1, 3, 7 and 21, whereas for $q = 2^4$, the branch splits into five subbranches in the ratio 1, 2, 4, 8 and 16. In both cases, the red and blue branches superimpose for $k = p\ell$ and $k' = q\ell, \ell \in \mathbb{Z}$.

asymptotic to $\theta = \pi/4$ is therefore the optimal solution with the smallest unit cell defined by

$$\begin{aligned} n &= 1 + \ell, m = \ell, \ell \in \mathbb{N}, \delta_\ell = \arctan \frac{\ell}{1 + \ell}, \\ \sigma_\ell &= 2\ell^2 + 2\ell + 1 \\ \sin \delta'_\ell &= \frac{1}{\sqrt{2\sigma_\ell}} \text{ with } \delta'_\ell = \frac{\pi}{4} - \delta_\ell \end{aligned} \quad (21)$$

with a primitive lattice defined by $A = (1 + \ell + i\ell)$, $B = [-\ell + i(1 + \ell)]$.

The case of the hexagonal system is treated in Appendix A and leads to

$$\begin{aligned} n &= 1 + 2\ell, m = \ell, \ell \in \mathbb{N}, \delta_\ell = \arctan \frac{\ell\sqrt{3}}{3\ell + 2}, \\ \sigma_\ell &= 3\ell^2 + 3\ell + 1 \\ \sin \delta'_\ell &= \frac{1}{2\sqrt{\sigma_\ell}} \text{ with } \delta'_\ell = \frac{\pi}{6} - \delta_\ell. \end{aligned} \quad (22)$$

These results are easily understood by noting that the smallest coincidence angles are obtained when the two superimposed nodes are as close as possible to each other.

Indeed, applying relation (4) to the rectangle system with $\theta = \pi/2$ and $n = 1, m = q\ell$ leads to

$$\sqrt{\sigma} \sin |\delta| = |-1| = 1. \quad (23)$$

For the square system with $\theta = \pi/4$ and $n = \ell + 1, m = \ell$, relation (4) gives

$$\sqrt{\sigma} \sin |\delta| = \frac{1}{\sqrt{2}} |\ell - \ell - 1| = \frac{1}{\sqrt{2}}, \quad (24)$$

and for the hexagonal system, with $\theta = \pi/6$ and $n = 2\ell + 1, m = \ell$

$$\sqrt{\sigma} \sin |\delta| = \frac{1}{2} |2\ell - 2\ell - 1| = \frac{1}{2}. \quad (25)$$

3. Space groups of homophase bilayers with coincidence lattices

Building the space group of a homophase bilayer with a coincidence lattice is a simple work in principle that follows the same general scheme: the symmetry group of a set of two identical objects taken as a whole is the union of the symmetry elements that are common to both objects and are intrinsic symmetries of these objects plus extra elements, if any, that exchange the two objects as illustrated in Fig. 9.

It is easily demonstrated that the union of these two sets forms a group (see, for instance, Gratias & Quiquandon, 2020). Here, both the rotation α and the rigid-body translations τ are to be considered in the computations of these two basic sets:

(i) The intersection group contains those symmetry elements of the original layers that are of the same nature and superimpose in space,

$$\mathcal{I} = \mathcal{G} \cap \mathcal{G}',$$

where $\mathcal{G}' = \widehat{\mathbf{a}} \mathcal{G} \widehat{\mathbf{a}}^{-1}$; this group is never empty since it contains at least the identity and the translation group \mathcal{T}_α of the coincidence lattice.

(ii) The additional set of symmetry elements correspond to those extra new elements that exchange the two layers, transforming layer I into II and simultaneously II into I , defined by the intersection of the cosets $\widehat{\mathbf{a}} \mathcal{G}$ with $\mathcal{G} \widehat{\mathbf{a}}^{-1}$ designated, if not empty, the exchange set \mathcal{E} :

$$\mathcal{E} = \widehat{\mathbf{a}} \mathcal{G} \cap \mathcal{G} \widehat{\mathbf{a}}^{-1}.$$

The symmetry group of the homophase bilayer, say \mathcal{N} of translation group \mathcal{T}_α , is thus the union

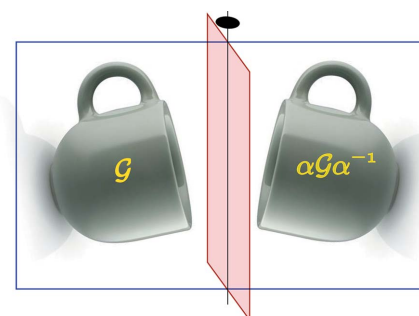
$$\mathcal{N} = \mathcal{I} \cup \mathcal{E} \text{ with either } \mathcal{E} = \emptyset \text{ or } \mathcal{E} = \widehat{\varepsilon} \mathcal{I} \text{ such that } \widehat{\varepsilon}^2 \in \mathcal{I}.$$

In addition to the group \mathcal{N} , another fundamental symmetry group of interest is the space group \mathcal{W}_α which generates, for a given rotation α and a given rigid-body translation τ , all translations τ' that generate equivalent bilayers, *i.e.* bilayers that can superimpose on top of each other by an isometry. Any two such translations τ and τ' for the same rotation α are said to be equivalent. They form the orbit of τ in \mathcal{W}_α .

Because the rigid-body translation acts as a global translation of the layers, it is sufficient to consider only the orientational symmetry, *i.e.* the point group Γ , instead of the whole space group \mathcal{G} . The point group W_α is obtained as in the preceding case, by considering the intersection of the point groups I and II and the exchange set but with the major change that, since the elements of the exchange set transform τ into its opposite, we must multiply the exchange set by the inversion operation:

$$W_\alpha = (\Gamma \cap \alpha \Gamma \alpha^{-1}) \cup (\bar{1})(\alpha \Gamma \cap \Gamma \alpha^{-1}), \quad (26)$$

where $\bar{1}$ stands for the inversion operator. [A very unfortunate mistake is to be corrected in the work of Gratias & Quiquandon (2020) where the inversion operation has been forgotten in the expression of W_α and improperly added in the one of \mathcal{N} .] Here again, it is easily shown that W_α is a group.



$$\mathcal{I} = \mathcal{G} \cap \widehat{\mathbf{a}} \mathcal{G} \widehat{\mathbf{a}}^{-1} \quad \mathcal{E} = \widehat{\mathbf{a}} \mathcal{G} \cap \mathcal{G} \widehat{\mathbf{a}}^{-1}$$

Figure 9

These two identical cups share the same mirror (blue frame) and transform into each other by another mirror (red frame) perpendicular to the previous one. Alone, each cup has the point symmetry m , but the pair of cups, taken as a whole, has point symmetry $2mm$.

The translation subgroup of \mathcal{W}_α is found owing to the fact that adding to τ any translation of the lattices of either crystal transforms the bilayer into one of its equivalents. This translation group is the union group \mathcal{U}_α introduced in Section 2.2.3. The set of equivalent translations to τ is therefore the orbit of τ in the space group $\mathcal{W}_\alpha(\mathcal{U}_\alpha)$ generated by the product of W_α with the translation group \mathcal{U}_α :

$$\mathcal{W}_\alpha(\mathcal{U}_\alpha) = W_\alpha \times \mathcal{U}_\alpha. \quad (27)$$

Hence, the number of different symmetry groups of the bilayers induced by varying the rigid-body translation τ for a given rotation α is the number of strata of the group $\mathcal{W}_\alpha(\mathcal{U}_\alpha)$. For example, as shown in Appendix A and Fig. 13, there are only six different space groups for graphene bilayers whatever the rigid-body translation (and whatever the α rotation). It also shows that the natural reference frame to be used for labeling τ is the union lattice. Moreover, the domain of definition of the rigid-body translation τ becomes very narrow and decreases linearly as $1/\sqrt{\Sigma}$ for coincidence angles α tending towards zero. As a consequence, at very small angles of rotation where the coincidence lattice unit cell increases dramatically, the unit cell of the union lattice becomes small enough for the rigid-body translation to become physically meaningless. Therefore, in the case of large moiré patterns due to small disorientations, it is not necessary to consider the rigid-body translation in the description (it can be chosen to be the null vector).

3.1. Finding the bilayer groups: point symmetry

The point symmetry elements to consider are rotations $z \rightarrow z \exp(i\phi)$ and mirrors $z \rightarrow \bar{z} \exp(2i\theta)$ with $\phi, \theta \in \{0, \frac{\pi}{6}, \frac{\pi}{4}, \frac{\pi}{3}, \frac{\pi}{2}\}$.

The rotation α commutes with all the rotations of the lattice crystal since

$$z \rightarrow z \exp(i\alpha) \exp(i\phi) = z \exp[i(\alpha + \phi)] = z \exp(i\phi) \exp(i\alpha).$$

The intersection point group $\Gamma \cap \alpha\Gamma\alpha^{-1}$ is thus the set of all the rotations of the point group of the crystal whatever the value of the coincidence angle α .

On the other hand, the exchange set $\alpha\Gamma \cap \Gamma\alpha^{-1}$ contains the mirrors generated by the product of the rotation α by the original mirrors, *i.e.* mirrors rotated by $\delta = \alpha/2$ from the original ones. Indeed, the elements of $\alpha\Gamma$ act on z as $z \rightarrow \exp(i\alpha)\bar{z} \exp(2i\theta) = \bar{z} \exp[i(\alpha + 2\theta)]$ whereas those of $\Gamma\alpha^{-1}$ act as $z \rightarrow \bar{z} \exp(-i\alpha) \exp(2i\theta) = \bar{z} \exp[i(\alpha + 2\theta)]$.

Therefore the exchange sets contain all the mirrors obtained by a rotation of $\delta = \alpha/2$ of the original mirrors of the structure whatever the value of the coincidence angle α . This explains why the coincidence lattice \mathcal{T}_α has the same point symmetry as the original symmetry class of the lattice. For the group W_α , the exchange set that contains all the mirrors is multiplied by the inversion, generating thus an equivalent set of mirrors but rotated by $\pi/2$ with respect to the initial ones.

3.2. Finding the bilayer groups: space symmetry

The space group \mathcal{W}_α is easily determined since it is the direct product of W_α with \mathcal{U}_α .

Concerning the group \mathcal{N} , the calculation requires a few steps.

Elements of \mathcal{I} are the elements $\hat{\mathbf{g}}, \hat{\mathbf{g}}' \in \mathcal{G}$ such that $\hat{\mathbf{a}}\hat{\mathbf{g}} = \hat{\mathbf{g}}'\hat{\mathbf{a}}$ and elements of \mathcal{E} are the elements $\hat{\mathbf{a}}\hat{\mathbf{g}}$ such that $\hat{\mathbf{a}}\hat{\mathbf{g}} = \hat{\mathbf{g}}'\hat{\mathbf{a}}^{-1}$.

From $\hat{\mathbf{a}}z = z \exp(i\alpha) + \tau$ and $\hat{\mathbf{a}}^{-1}z = z \exp(-i\alpha) - \tau \exp(-i\alpha)$, with $\hat{\mathbf{g}}$ being either a rotation $\hat{\mathbf{g}}z = z \exp(i\phi) + t$, or a mirror $\hat{\mathbf{g}}z = \bar{z} \exp(2i\theta) + t$, we have the general explicit expressions

$$\hat{\mathbf{a}}\hat{\mathbf{g}}z = \begin{cases} \exp(i\alpha)[z \exp(i\phi) + t] + \tau = z \exp[i(\alpha + \phi)] \\ + t \exp(i\alpha) + \tau \\ \exp(i\alpha)[\bar{z} \exp(2i\theta) + t] + \tau = \bar{z} \exp[i(\alpha + 2\theta)] \\ + t \exp(i\alpha) + \tau \end{cases} \quad (28)$$

$$\hat{\mathbf{g}}\hat{\mathbf{a}}z = \begin{cases} [z \exp(i\alpha) + \tau] \exp(i\phi) + t = z \exp[i(\alpha + \phi)] \\ + t \exp(i\phi) + t \\ [\bar{z} \exp(-i\alpha) + \bar{\tau}] \exp(2i\theta) + t = \bar{z} \exp[i(2\theta - \alpha)] \\ + \bar{\tau} \exp(2i\theta) + t \end{cases} \quad (29)$$

$$\hat{\mathbf{g}}\hat{\mathbf{a}}^{-1}z = \begin{cases} [z \exp(-i\alpha) - \tau \exp(-i\alpha)] \exp(i\phi) + t \\ = (z - \tau) \exp[i(\phi - \alpha)] + t \\ [\bar{z} \exp(i\alpha) - \bar{\tau} \exp(i\alpha)] \exp(2i\theta) + t \\ = (\bar{z} - \bar{\tau}) \exp[i(\alpha + 2\theta)] + t. \end{cases} \quad (30)$$

For an element being possibly included in either set \mathcal{I} or \mathcal{E} , the arguments of the variable z must be identical for the equalities to hold for any value of z .

Concerning \mathcal{I} , the comparison between the lines (28) and (29) shows that the only possible solution for the elements $\hat{\mathbf{g}}$ and $\hat{\mathbf{g}}'$ to be in \mathcal{I} is two rotations of the same angle ϕ such that

$$t' - t \exp(i\alpha) = \tau - \tau \exp(i\phi).$$

Concerning \mathcal{E} , the comparison of (28) with (30) shows that the pertinent elements $\hat{\mathbf{a}}\hat{\mathbf{g}}$ are obtained with $\hat{\mathbf{g}}$ and $\hat{\mathbf{g}}'$ being parallel mirrors such that

$$t' - t \exp(i\alpha) = \tau + \bar{\tau} \exp(i\alpha) \exp(2i\theta) = \tau + \bar{\tau} \exp[2i(\theta + \delta)]$$

with $t, t' \in \mathcal{U}_\alpha$ or possibly $\mathcal{U}_\alpha/2$ for the *c*-type space groups *cm* and *c2mm* and the non-symmorphic ones *pg*, *p2mg*, *p2gg* and *p4gm*.

Since $t' - t \exp(i\alpha)$ is a vector of \mathcal{U}_α or $\mathcal{U}_\alpha/2$, we find that:

(i) The rotation $(\phi|t) \in \mathcal{G}$ is in \mathcal{I} if τ is such that $\tau - \tau \exp(i\phi)$ is a vector of \mathcal{U}_α (or $\mathcal{U}_\alpha/2$) which is achieved for τ pointing to special positions of the group \mathcal{W}_α .

(ii) The mirror $(m_{\theta+\delta}|t)$ is in \mathcal{E} if τ is such that $\tau + \bar{\tau} \exp[2i(\theta + \delta)]$ is a vector of \mathcal{U}_α or $\mathcal{U}_\alpha/2$ requiring thus τ to point along the perpendicular bisector of a mirror of \mathcal{E} and thus τ to align along a mirror of \mathcal{W}_α .

These two conditions lead to non-trivial solutions for τ being located at special positions of $\mathcal{W}_\alpha(\mathcal{U}_\alpha)$.

This shows that the space group \mathcal{N} depends on the value of τ according to the different symmetry strata of $\mathcal{W}_\alpha(\mathcal{U}_\alpha)$: the number of different possible space groups

of the bilayer is equal to the number of symmetry strata of the group $\mathcal{W}_\alpha(\mathcal{U}_\alpha)$.

Moreover, the type of space group \mathcal{N} of the bilayer does not depend on the value of the coincidence angle α : whatever the value of α in that set is, the groups \mathcal{N} obtained for rigid-body translations τ with the same coordinates in \mathcal{U}_α are isosymbolic; their actual representations in space are scaled according to the length $\sqrt{\sigma}$ and the rotation $\delta = \alpha/2$.

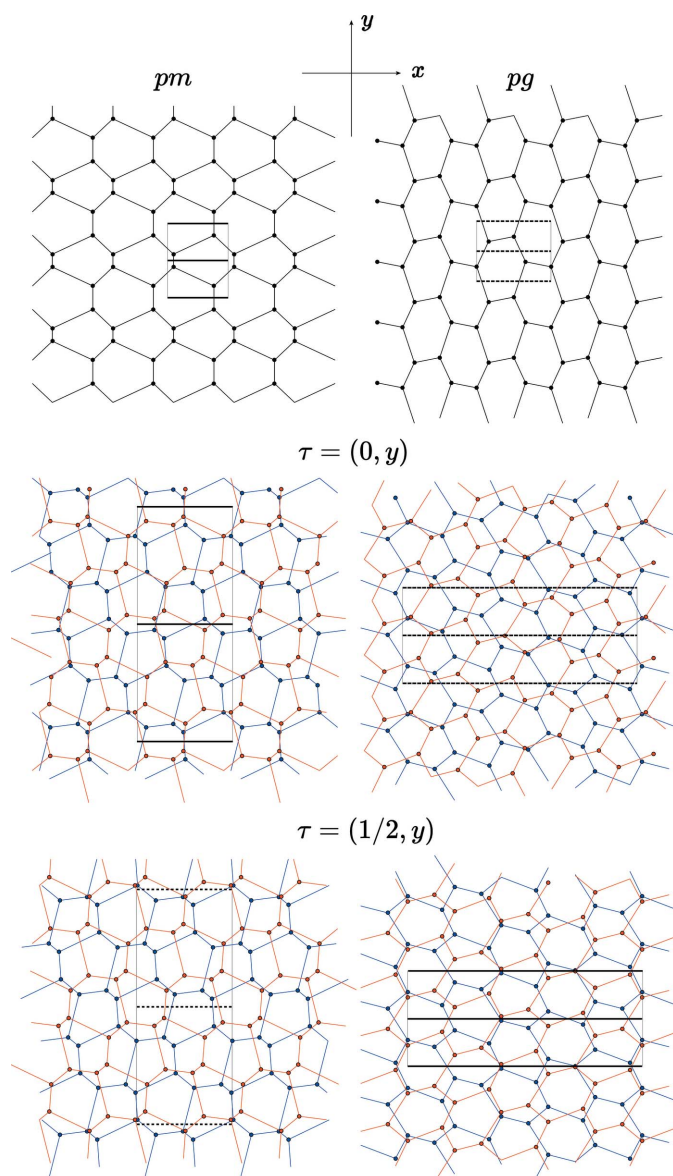


Figure 10
 Example of structures of symmetry $pm_x(\Lambda)$ and $pg_x(\Lambda)$, showing that the mirror of the exchange set survives in the bicrystal symmetry only for the rigid-body translation τ located at special positions of the group $\mathcal{W}_\alpha = pm_y$, with translation group \mathcal{U}_α . Beyond the general position (x, y) generating a bilayer of symmetry $p1$ and not shown here, there are two other strata $(0, y)$ and $(1/2, y)$ which generate a mirror in the bilayer structure. According to the values 0 or $1/2$ of the x component of τ on \mathcal{U}_α , these mirrors are either pure or glide. Here $\rho = \sqrt{3}/2$, $n = 1$, $m = 1$, $\alpha = 101.537^\circ$; the coincidence lattice \mathcal{T}_α is defined by $T_1 = (1, 1)$, $T_2 = (3, 2)$ with $\Sigma = 5$.

3.3. A simple low-symmetry example

We consider two bilayers A and B with coincidence lattices built from structures of symmetry class m_x with space groups $pm_x(\Lambda)$ for A and $pg_x(\Lambda)$ for B . In both cases, the point group W_α is made of the identity for the intersection group and m_y (original m_x rotated by $\delta = \alpha/2$ plus $\pi/2$ because of the inversion) for the exchange set: $\mathcal{W}_\alpha = pm_y$ with translation group \mathcal{U}_α . This group has three strata expressed in the unit cell of \mathcal{U}_α : $(0, y)$, $(1/2, y)$ and (x, y) with little groups, respectively, m_y , m_y and 1. The translation $\tau = (0, y)$ expressed in the unit cell of \mathcal{U}_α generates the group $\mathcal{N} = pm_x$ for the structure A and $\mathcal{N} = pg_x$ for structure B , both of translation group \mathcal{T}_α , and vice versa for the translation $\tau = (1/2, y)$ (Fig. 10).

4. Conclusion

To summarize, we find that infinitely many coincidence lattices generically exist down to the rectangle symmetry provided that the ratio ρ of the lengths of the unit-cell vectors is the square root of a rational number: $\rho^2 = p/q$. They are generated by specific coincidence rotations of angle α of the form $\alpha = 2\delta = 2 \arctan(\rho m/n)$ where n and m are coprime integers and can be written as

$$\mathcal{T}_\alpha = \exp(i\delta)\sqrt{\sigma}\left(N + i\rho\frac{q}{\gamma}M\right), N, M \in \mathbb{Z},$$

where $\sigma = n^2 + \rho^2 m^2$ and $\gamma = \text{gcd}(mp, nq)$.

With each coincidence lattice is associated a union lattice

$$\mathcal{U}_\alpha = \mathcal{T}_\alpha / \Sigma$$

homothetic to \mathcal{T}_α and which is the translation group of the space group of the equivalent translations of the rigid-body translation τ . Both coincidence and union lattices share at least the symmetry class of the original layer. For square and hexagonal systems, the three lattices \mathcal{T}_α , Λ and \mathcal{U}_α are two-by-two homothetic in the linear ratio $\sqrt{\Sigma}$.

The complete set of possible coincidence lattices characterized by the rotation angle α and the unit-cell size Σ of the corresponding coincidence lattice form a diagram in one-to-one correspondence with the so-called set of points visible from the origin and can be analyzed using Farey sequences. They are distributed on branches, each characterized by a geometric invariant relating the sinus of the rotation angle to the square root of the unit-cell size.

In the case where a coincidence lattice exists, the space group of the bilayer depends on the value of the rigid-body translation τ between the two layers. There are as many different symbolic names of space groups as there are strata in the group $\mathcal{W}_\alpha(\mathcal{U}_\alpha)$ of the equivalent translations τ to a given one. These symbolic names do not depend on the value of the rotation α .

Because the group $\mathcal{W}_\alpha(\mathcal{U}_\alpha)$ has \mathcal{U}_α as translation subgroup, the unit-cell size of which tends to zero for rotations tending to zero, the rigid-body translation τ becomes a non-pertinent parameter – analogous to a phason field in quasicrystals – for twisted bilayers with very small rotation.

A subsequent work will discuss the case of general bilayers where \mathcal{U}_α is a \mathbb{Z} module of rank 4 in connection with the notion of 0-lattice which is independent of the possible existence of a coincidence lattice.

APPENDIX A

The specific example of graphene bilayers

Graphene has a 2D periodic structure of group $p6mm(\mathbf{a}, \mathbf{b})$ with a carbon atom at special position $2b\ 3m(1/3, 2/3)$. It is described in the complex plane \mathbb{C} by the primitive hexagonal lattice Λ ($\rho = 1, \varphi = 2\pi/3$) defined by

$$\Lambda = \{z = n + jm, j = \exp(2i\pi/3), n, m \in \mathbb{Z}\}$$

with a carbon atom at position $z_1 = (1 + 2j)/3$ [and equivalently $z_2 = (2 + j)/3$] as shown in Fig. 11(a). [It turns out that the commonly used notation in the physics community of graphene is to take the hexagonal reference frame with the acute angle $\pi/3$ instead of the crystallographic definition that uses the angle $2\pi/3$. This corresponds to choosing $(-\bar{j}, 1)$ as reference frame instead of $(1, j)$. Noting thus that a node z can be equivalently written as $z = n + mj = M - N\bar{j}$ we obtain $n = N + M$ and $m = N$ and thus $M = n - m$.] The unit-cell parameter equal to $a = 0.2456$ nm is chosen here as the unit length.

The point symmetry elements of $6mm$ are generated by the rotation of $\pi/3$ located at the origin and transforming (the six hexagonal rotations are $\{1, -\bar{j}, j, -1, \bar{j}, -j\}$) z into $-\bar{j}z$ and the mirror along x transforming z into \bar{z} . The orbit G_z of a generic point z has thus 12 elements per unit cell:

$$G_z = \{z, -\bar{j}z, jz, -z, \bar{j}z, -jz, \bar{z}, -j\bar{z}, \bar{j}\bar{z}, -\bar{z}, j\bar{z}, -\bar{j}\bar{z}\} + \Lambda$$

as exemplified in Fig. 11(b).

A1. Graphene bilayers with coincidence lattices

Twisted graphene bilayers are certainly among the most studied materials in the world [see, for instance, the recent review by Geim (2009)], often created, for example, in epitaxial graphene growth on the C-terminated face of Si-C (see Campanera *et al.*, 2007; Hass *et al.*, 2008; Varchon *et al.*, 2008; Bistritzer & MacDonald, 2011). These twisted bilayers are the superimposition of two single graphene sheets slightly twisted with respect to each other by a small angle α of a few degrees or less. It was seen a couple of years ago that these twisted graphene bilayers have remarkable electronic structures (see Trambly de Laissardière *et al.*, 2010). As already mentioned, from the geometric point of view discussed here, the two graphene sheets are considered as infinitely thin and located on the same plane.

Twist rotations of angle α leading to coincidence lattices are infinitely many (see Feuerbacher, 2021). They are characterized by the rotations α that superpose a representative of a given orbit of nodes $z = n + jm$ on top of another point of the same orbit G_z . As previously mentioned, because of the high symmetry of the hexagonal system, it is enough to examine the

rotation $\alpha = 2\delta$ around the origin that transforms the lattice point $z = n + \bar{j}m = n - m - jm$ into $z' = n + jm$ as shown in Fig. 11, where n and m are positive coprime integers with $n > 2m > 0$:

$$n + \bar{j}m \xrightarrow{\alpha} n + jm = \exp(i\alpha)(n + \bar{j}m) \tag{31}$$

or

$$\exp(i\alpha) = \frac{n + jm}{n + \bar{j}m} = \left(\frac{n + jm}{\sqrt{\Sigma}}\right)^2 \text{ and thus}$$

$$\sqrt{\Sigma} \exp(i\delta) = n + jm,$$

where $\delta = \alpha/2$ and $\Sigma = n^2 + m^2 - nm$, as application of equation (7) to the hexagonal system.

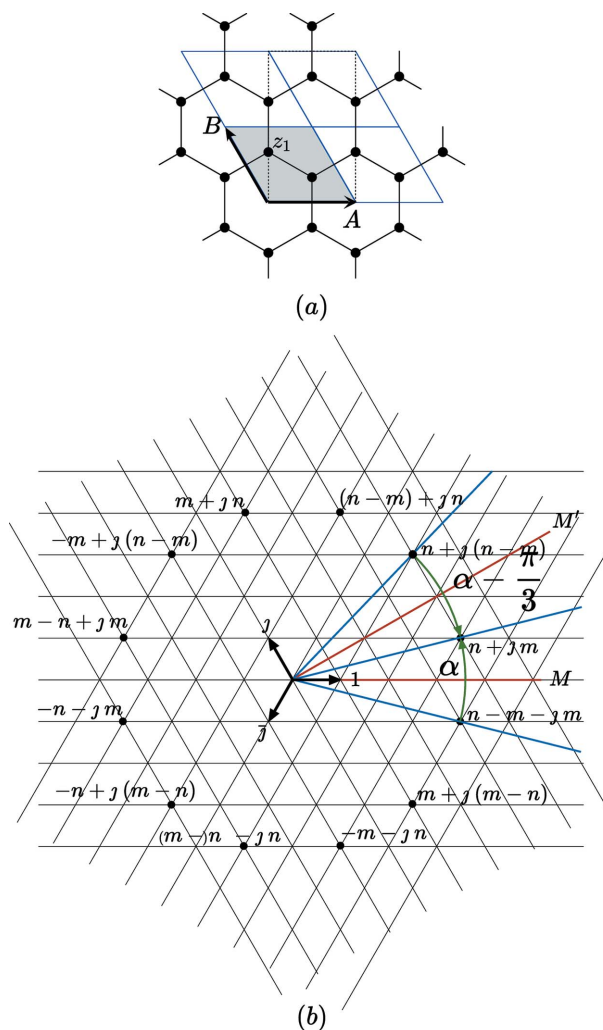


Figure 11 (a) Graphene is a 2D structure made of a honeycomb lattice of carbon atoms (in black on the picture). The standard primitive hexagonal lattice is generated by the pair $1, j = \exp(2i\pi/3)$ in complex notations defining the unit cell drawn in gray. The point symmetry group is $6m$ which can be generated by the two mirrors M and M' . (b) Generating coincidence lattices by rotation is easily obtained by applying rotations α around the origin that superpose nodes deduced from each other by the mirror along the real axis transforming the node $n + \bar{j}m$ into $n + jm$. Because of the hexagonal symmetry, choosing point $n + \bar{j}m$ with n, m coprime in the region $n > 2m > 0$ between the mirrors M and M' is sufficient for generating all the possible rotations of coincidence angles α and $\pi/3 - \alpha$.

A2. Hexagonal and rectangular coordinates

The connection between the rectangular c -type lattice with $\rho = \sqrt{3}$ reference frame with coordinates (n_r, m_r) both integers or both half-integers and the hexagonal lattice reference frame (n_h, m_h) both integers is given by

$$\begin{cases} n_h = n_r + m_r, \\ m_h = 2m_r, \end{cases} \quad \begin{cases} 2n_r = 2n_h - m_h \\ 2m_r = m_h. \end{cases}$$

It is easily verified that σ is an integer for both n_r and m_r being half-integers,

$$\begin{aligned} \sigma &= n_r^2 + 3m_r^2 = \left(N + \frac{1}{2}\right)^2 + 3\left(M + \frac{1}{2}\right)^2 \\ &= N^2 + N + \frac{1}{4} + 3M^2 + 3M + \frac{3}{4} \\ &= N(N + 1) + 3M(M + 1) + 1, \end{aligned}$$

and that

$$\begin{aligned} \Sigma &= n_h^2 + m_h^2 - n_h m_h \\ &= (n_r + m_r)^2 + 4m_r^2 - 2m_r(n_r + m_r) \\ &= n_r^2 + 3m_r^2 = \sigma. \end{aligned}$$

{The relation $\Sigma = q\sigma/\gamma$, found for the rectangular system, is based on $\gamma = \gcd(m_r, n_r) = \gcd(3m_r, n_r) = \gcd(3, n_r)$ and leads to $\gamma = 1$ – and thus $\Sigma = \sigma$ as expected – when n_r is not a multiple of 3, but to $\gamma = 3$ when $n_r = 3h_r$ and thus $\Sigma = \sigma/3$ which seems contradictory to the present result. In fact, because $n_h = 3h_r + m_r, m_h = 2m_r$, the sum $n_h + m_h$ is a multiple of 3 and the actual coincidence unit cell reduces to $[(n_h + m_h)/3, (2m_h - n_h)/3]$, which is indeed three times smaller.}

A3. Coincidence and union lattices

Relation (6) leads to

$$\delta = \arctan \frac{m\sqrt{3}}{2n - m} \tag{32}$$

and

$$2\sqrt{\Sigma} \sin \delta = m\sqrt{3}, \quad 2\sqrt{\Sigma} \cos \delta = 2n - m. \tag{33}$$

The unit vectors of \mathcal{T}_α are $T_1 = n + jm$ and $T_2 = jT_1 = -m + j(n - m)$; because of relation (33), this translates into $T_1 = \exp(i\delta)\sqrt{\Sigma}$ and since $T_2 = jT_1$:

$$T_\alpha = \exp(i\delta)\sqrt{\Sigma}(N + jM), \quad N, M \in \mathbb{Z}. \tag{34}$$

The coincidence lattice \mathcal{T}_α is an hexagonal lattice deduced from the original lattice Λ of the layer by a rotation of δ with unit-cell parameter $\sqrt{\Sigma}$. The calculation of the union lattice \mathcal{U}_α leads to the same expression as in equation (10):

$$\mathcal{U}_\alpha = \mathcal{T}_\alpha / \Sigma$$

which is the original hexagonal lattice rotated by δ with a unit-cell parameter linearly shrunk by $1/\sqrt{\Sigma}$.

A4. The coincidence pattern \mathcal{P}

The coincidence pattern is shown in Fig. 12, generated by one unique representative out of the 12 equivalents of the rotation, with the corresponding Σ plotted on a logarithmic scale. As already discussed in Section 2.3, the coincidence points are distributed on branches converging asymptotically to specific rotation values when $\Sigma \rightarrow \infty$. Putting $n_{k,k'} = kn_0 + k'n_1$ and $m_{k,k'} = km_0 + k'm_1$ from equation (14), we obtain

$$\begin{cases} \alpha_{k,k'} &= 2 \arctan \left[\sqrt{3} \frac{km_0 + k'm_1}{2(kn_0 + k'n_1) - (km_0 + k'm_1)} \right] \\ \Sigma_{k,k'} &= k^2\sigma_0 + k'^2\sigma_1 + kk'\beta' \end{cases} \tag{35}$$

with $\beta' = 2(n_0n_1 + m_0m_1) - (m_1n_0 + m_0n_1)$. The basic invariance relations (13) for each branch are in hexagonal coordinates:

$$\begin{aligned} k' = \text{Cte} : \forall k \in \mathbb{Z}, \quad 2\sqrt{\sigma_{k,k'}}\sigma_0 \sin \delta_{(k,k'),0} &= k'\sqrt{3} \\ k = \text{Cte} : \forall k' \in \mathbb{Z}, \quad 2\sqrt{\sigma_{k,k'}}\sigma_1 \sin \delta_{1,(k,k')} &= k\sqrt{3}, \end{aligned} \tag{36}$$

where Cte stands for a constant value. Here, again, the optimal branches are those where $k'(k) = 1$ for running $k(k')$ drawn in cyan and red in Fig. 12. Of greatest importance are the optimal branches associated with the nodes of the initial Farey sequence $F_h(2) = [(1, 0), (2, 1)]$ since they cover the entire angular definition domain of \mathcal{P} generating the smallest Σ values. We find

$$\sigma_0 = 1, \quad \sigma_1 = 3$$

$$n_{k,1} = 2 + k, \quad m_{k,1} = 1, \quad \sigma_{k,1} = k^2 + 3k + 3$$

$$n_{1,k'} = 1 + 2k', \quad m_{1,k'} = k', \quad \sigma_{1,k'} = 3k'^2 + 3k' + 1$$

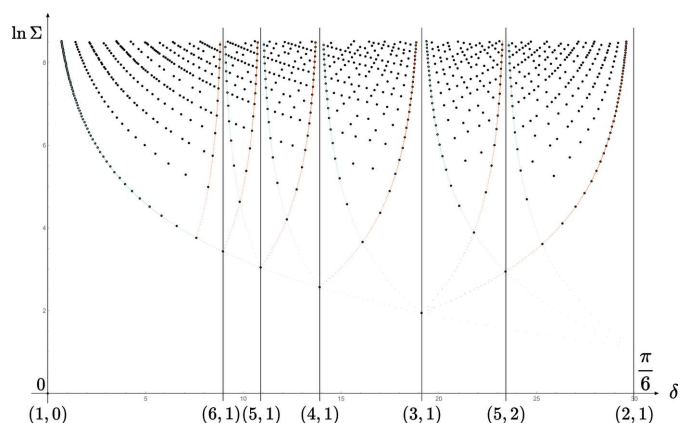


Figure 12
The rotations of coincidence $n + jm \rightarrow n + jm$ are defined by $\delta = \arctan m\sqrt{3}/(2n - m)$ $n, m \in \mathbb{Z}, n > 2m > 0$ plotted for one unique twist rotation as a function of $\Sigma = n^2 + m^2 - nm$ for $\Sigma < 8000$, on a logarithmic scale. As in the general case, well defined asymptotic branches are observed which correspond to the terms of the consecutive Farey sequences: the asymptotic branches of the $F_h(6)$ sequence are drawn in cyan and red.

$$\sin \delta_{k,1} = \frac{\sqrt{3}}{2\sqrt{k^2 + 3k + 3}} \text{ for } \alpha \rightarrow 0$$

$$\sin \delta_{1,k'} = \frac{1}{2\sqrt{3k'^2 + 3k' + 1}} \text{ for } \alpha \rightarrow \pi/3.$$

The same δ angle is found between the two branches for $k = 3k'$ with $\sigma_{k,1} = 3\sigma_{1,k'}$. Indeed, since then $n_{k,1} = 2 + 3k'$ we see that $n_{k,1} + m_{k,1} = 3(1 + k')$ and, of course, $n_{k,1} - 2m_{k,1} = 3k'$ are both multiples of 3, leading to a unit cell three times smaller. This shows that the asymptotic branch $\delta \rightarrow \pi/6$ is the optimal solution leading to the smallest unit cells:

$$n = 1 + 2\ell, \quad m = \ell, \quad \ell \in \mathbb{N}, \quad \sigma_\ell = 3\ell^2 + 3\ell + 1$$

with $\sin \delta_\ell = \frac{1}{2\sqrt{\sigma_\ell}}$.

A5. Symmetry groups of twisted graphene bilayers

Our last task is to analyze the overall symmetry of the graphene twisted bilayers with coincidence lattices. The group $\mathcal{W}_\alpha(\mathcal{U}_\alpha)$ is easily found as $\mathcal{W}_\alpha(\mathcal{U}_\alpha) = p6mm$ of translation group \mathcal{U}_α whatever the value of the coincidence angle δ in \mathcal{P} . The group $p6mm$ contains six symmetry strata listed in Table 3. There are thus only six different possible space groups for the bilayer according to the coordinates of τ expressed in units of the union lattice \mathcal{U}_α as shown in Table 3 and exemplified in Fig. 13.

Table 3

Symmetry groups \mathcal{N} of graphene twisted bilayers as a function of the rigid-body translation τ expressed on the basis of the union group $\mathcal{W}_\alpha(\mathcal{U}_\alpha) = p6mm'$ with origin chosen on the sixfold axis.

Its translation group is the union lattice \mathcal{U}_α defined by $U_1 = (n + jm)/\Sigma$ and $U_2 = [-m + j(n - m)]/\Sigma$ with $\Sigma = n^2 + m^2 - nm$.

	$\tau(\mathcal{U}_\alpha)$	Little group in $\mathcal{W}_\alpha(\mathcal{U}_\alpha)$	$\mathcal{N}_\tau(\mathcal{T}_\alpha)$	Label in Fig. 13
1a	(0, 0)	$6mm'$	$p6mm'$	(a)
2b	$(1/3, 2/3)^\dagger$	$3m'$	$p31m'$	(b)
3c	$(1/2, 0)$	$2mm'$	$c2mm'$	(c)
6d	$(x, 0)$	$.m'$	cm'	(d)
6e	(x, \bar{x})	$.m$	cm	(e)
12f	(x, y)	1	$p1$	(f)

† The rigid-body translation $\tau = (1/3, 2/3)$ corresponds to the natural stacking in graphite.

The case of very small rotations deserves some attention. Rotations decreasing to zero are associated with coincidence lattices with larger and larger unit cells and therefore to shorter unit cells for the union lattices. As noticed in the body of the text, this leads to rigid-body translations tending to zero and therefore losing any physical pertinence. Small rotations can indeed be locally described as translations between the two almost-parallel layers, as shown in Fig. 14(a). The normalizer at $\tau = 0$ is the group of the graphene layer, $p6mm$, scaled by $\sqrt{\Sigma}$ and rotated by δ : the bilayer has exactly the same symmetry properties as the initial graphene unit cell but magnified to mesoscopic scales. It can be roughly described as

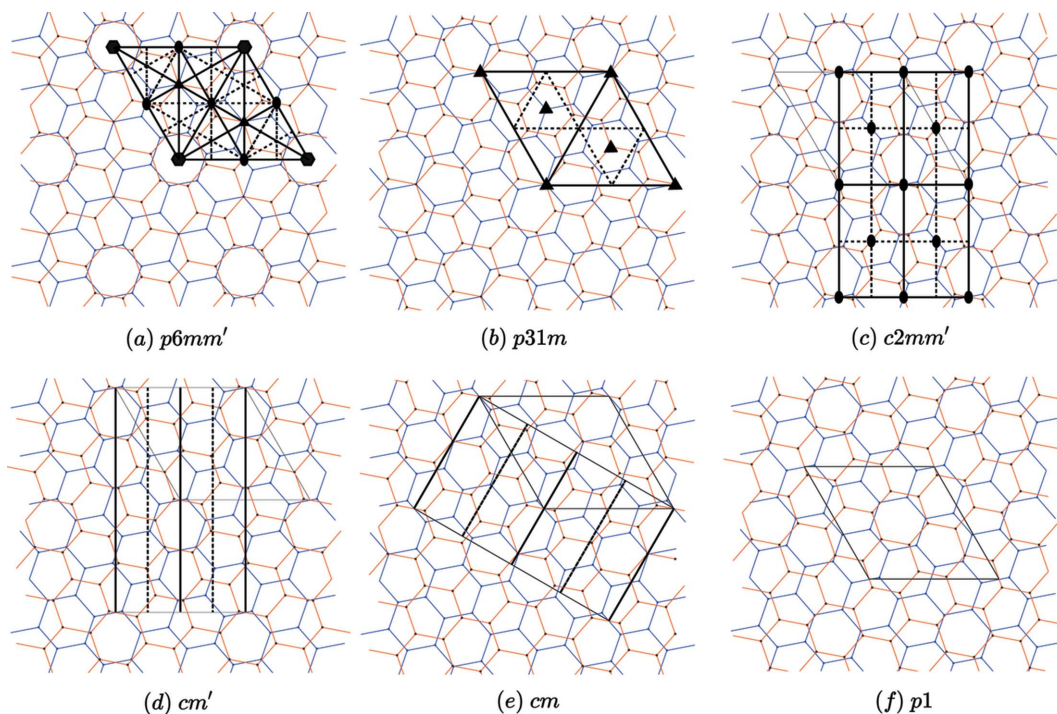


Figure 13

Example of a graphene bilayer with twist rotation $(n, m) = (3, 1)$, $\alpha = 2 \arctan \sqrt{3}/5 = 38.2132^\circ$, $T_1 = (-1, -2)$, $T_2 = (2, 3)$, $\Sigma = 7$, as a function of the rigid-body translation τ shown in Table 3. All coincidence angles α in \mathcal{P} generate symmetry groups with the same symbols; they differ only by the scaling factor defined by the union and coincidence lattices.

an hexagonal tiling made of three main microscopic high-symmetry structures occurring at each special point of the large hexagonal coincidence unit. In that renormalization-like view, the centers of the initial hexagons are replaced by the structure of local symmetry $6mm$, usually designated as AA , that is the graphene itself, the carbon atoms by the structure of local symmetry $3m$, called $AB(BA)$, as in the natural graphite, and the binding between carbon atoms, designated as SP , by the structure $2mm$ shown in Fig. 14(b) of space group $c2m$ with cell parameters ($a = 1, b = \sqrt{3}$) and two carbon atoms at positions $(0, 1/3)$ and $(1/2, 1/3)$. These three basic high-symmetry structures, $6mm$, $3m$ and $2mm$, correspond to the first three special positions of dimension 0 as shown in Table 3 and Fig. 13. This exhausts all the symmetry possibilities: there are no other kinds of structures, for any $\delta \ll 1$ and any (here, meaningless) values of τ .

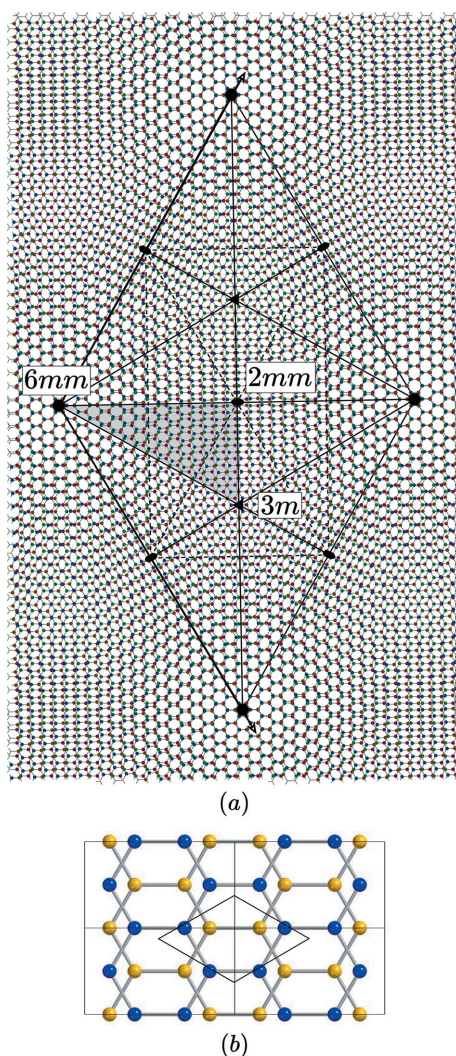


Figure 14
 (a) Small rotations 2δ generate bilayers with the same symmetry as the original graphene layer, magnified by $\sqrt{\Sigma}$ and rotated by δ . (b) Four unit cells of the local structure often called SP corresponding to the special point $2mm$.

APPENDIX B

Heterophase bilayers with coincidence lattices

B1. Homogeneous dilatation–rotation coincidence lattices for heterophase bilayers

Heterophase bilayers are formed by two layers of different structures; they show very similar geometrical properties to the homophase bilayers. However, our present context of using complex numbers allows us to treat here only those heterophase bilayers where the lattices Λ and Λ' of the layers can be deduced from each other by a dilatation–rotation, *i.e.* when

$$\Lambda' = \Delta\Lambda, \text{ where } \Delta = \varrho \exp(i\alpha), \varrho \in \mathbb{R}^+.$$

Here, ϱ is the dilatation coefficient and α the rotation from Λ to Λ' . This kind of transformation is the general case when the lattices belong both to either the square or the hexagonal systems as exemplified in Fig. 15.

We choose here to discuss heterophase bilayers in the square system for simplicity.

Let Λ and Λ' be the two square lattices of lattice parameters $a = 1$ for Λ and $a' = \varrho$ for Λ' :

$$\Lambda = \{n + im\}, n, m \in \mathbb{Z} \text{ and } \Lambda' = \varrho \exp(i\alpha)\{n' + im'\}, \\ n', m' \in \mathbb{Z}, \alpha \in \mathbb{R}.$$

A coincidence lattice $\mathcal{T} = \Lambda \cap \Lambda'$ exists if two pairs of integers (n, m) and (n', m') exist with $\gcd(n, m, n', m') = 1$ such that

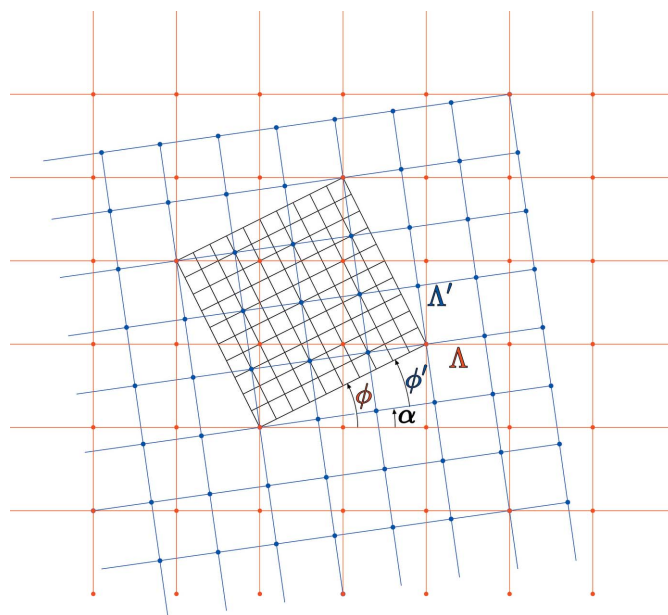


Figure 15
 Example of a bilayer made of two square lattices related by a dilatation–rotation operation inducing a coincidence lattice: here the node $(2, 1)$ of Λ (in red) is superimposed on the node $(3, 1)$ of Λ' (in blue). The coincidence lattice is thus $\mathcal{T}_\Lambda = \{(2, 1), (-1, 2)\}$, $\Sigma = 5$ expressed in the unit cell of Λ or equivalently $\mathcal{T}_{\Lambda'} = \{(3, 1), (-1, 3)\}$, $\Sigma' = 10$ expressed in the unit cell of Λ' ; the dilatation is $\varrho = 1/\sqrt{2}$ and the rotation $\alpha = \arctan 1/7 = 8.1301^\circ$.

$$n + im = \varrho \exp(i\alpha)(n' + im'), \quad (37)$$

in which case the coincidence lattice is $\{T_1 = n + im, T_2 = iT_1 = -m + in\}_\Lambda$ expressed on the unit cell of Λ or equivalently $\{T'_1 = n' + im', T'_2 = -m' + in'\}_{\Lambda'}$ expressed on the unit cell of Λ' . Explicitly

$$\varrho \exp(i\alpha) = \frac{n + im}{n' + im'} = \frac{nn' + mm' + i(n'm - m'n)}{n^2 + m^2}$$

or by putting $\Sigma = n^2 + m^2, \Sigma' = n'^2 + m'^2$, we obtain

$$\varrho = \sqrt{\frac{\Sigma}{\Sigma'}} \text{ and } \alpha = \arctan \frac{n'm - m'n}{nn' + mm'}. \quad (38)$$

Therefore, two square lattices (it can be easily verified that the same property applies for the case of hexagonal lattices) of different sizes can share a coincidence lattice only if the ratio of the unit-cell lengths is the square root of a rational number $\varrho^2 \in \mathbb{Q}^+$ in which case the area of the coincidence unit cell is simultaneously an integer multiple Σ of the area of the unit cell of the first lattice and another integer multiple, Σ' , of the unit cell of the second lattice in the ratio of the rational number $\varrho^2 = \Sigma/\Sigma'$.

Relation (37) leads to

$$\frac{n + im}{\sqrt{\Sigma}} = \exp(i\alpha) \frac{n' + im'}{\sqrt{\Sigma'}} \text{ or } \sqrt{\Sigma'}(n + im) = \exp(i\alpha)\sqrt{\Sigma}(n' + im').$$

Let ϕ and ϕ' be the rotation angles between the unit cell of the coincidence lattice \mathcal{T} and those of, respectively, Λ and Λ' (see Fig. 15); we have

$$\mathcal{T} = \sqrt{\Sigma} \exp(i\phi)\Lambda = \sqrt{\Sigma'} \exp(i\phi')\Lambda'$$

and therefore

$$\sqrt{\Sigma} \cos \phi = n, \quad \sqrt{\Sigma} \sin \phi = m, \quad \tan \phi = \frac{m}{n} \quad (39)$$

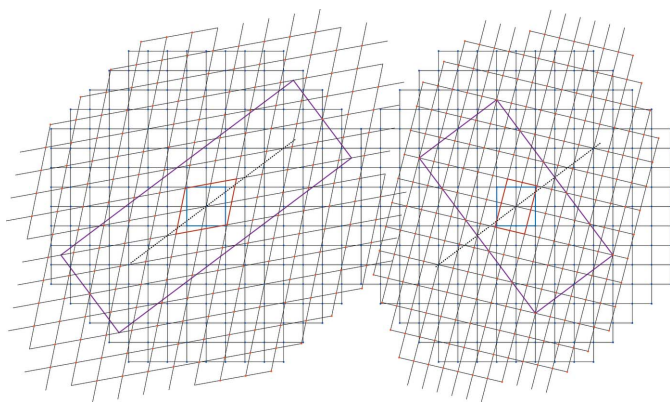


Figure 16
The square lattice in blue is transformed into the lattice in red after a rotation $\alpha = 2\arctan(1/3) = 36.8699^\circ$ (dashed lines) and (left) a dilatation $\zeta = 1/2$ with coincidence unit cell: $A = (12, 9), B = (-3, 4)$; (right) a shear $\eta = 1/2$ with coincidence unit cell: $A = (4, 3), B = (-6, 8)$.

$$\sqrt{\Sigma'} \cos \phi' = n', \quad \sqrt{\Sigma'} \sin \phi' = m', \quad \tan \phi' = \frac{m'}{n'}. \quad (40)$$

Also, because $\alpha = \phi - \phi'$:

$$\exp(i\alpha) = \frac{1}{\sqrt{\Sigma\Sigma'}} [nn' + mm' + i(n'm - m'n)]$$

or

$$\sqrt{\Sigma\Sigma'} \cos \alpha = nn' + mm', \quad \sqrt{\Sigma\Sigma'} \sin \alpha = n'm - nm'$$

which is consistent with the expression of α given by relation (38).

The union lattice $\mathcal{U} = \Lambda \cup \Lambda'$ is given by

$$\mathcal{U} = \frac{1}{\Gamma} \mathcal{T}, \text{ where } \Gamma = \frac{\Sigma\Sigma'}{\gcd(\Sigma, \Sigma') \gcd(n, m) \gcd(n', m')}.$$

It is easily checked that, in the homophase case, where $\Sigma = \Sigma', \gcd(n, m) = \gcd(n', m') = 1$, this relation simplifies to (10).

Fig. 15 gives a simple example of a rotation–dilatation transformation between two square lattices Λ, Λ' where the node $(n, m) = (2, 1)$ of Λ (in red) superimposes on the node $(n', m') = (3, 1)$ of Λ' (in blue) by a rotation α and a dilatation ϱ . Here $\Sigma = 1 + 4 = 5$ and $\Sigma' = 1 + 9 = 10$. Thus, we find $\varrho = \sqrt{5/10} = 1/\sqrt{2}$ and $\tan \alpha = (3 - 2)/(6 + 1) = 1/7$. We have $\tan \phi = 1/2$ with $\cos \phi = 2/\sqrt{5}, \sin \phi = 1/\sqrt{5}$ and $\tan \phi' = 1/3$ with $\cos \phi' = 3/\sqrt{10}$ and $\sin \phi' = 1/\sqrt{10}$.

B1.1. Pure dilatation. A pure dilatation of one layer with respect to the other is characterized by $\alpha = 0$ and therefore $nm' = mn'$ or $m/n = m'/n'$. We assume n and n' are non-zero, leading to

$$\Sigma = n^2(1 + m^2/n^2), \quad \Sigma' = n'^2(1 + m'^2/n'^2)$$

$$\sqrt{\frac{\Sigma}{\Sigma'}} = \sqrt{\frac{n^2}{n'^2}} = \frac{n}{n'}.$$

The union lattice $\mathcal{U} = \Lambda \cup \Lambda'$ is written

$$\mathcal{U} = \frac{\gcd^2(n, n')}{nn'} \mathcal{T}.$$

APPENDIX C

Homophase bilayer under mechanical deformation

The two layers can in general be of two different structures of space groups \mathcal{G} and \mathcal{G}' with lattices, respectively, Λ and Λ' . We still designate by $\hat{\mathbf{a}}$ the transformation from Λ to Λ' ,

$$\Lambda' = \hat{\mathbf{a}}\Lambda,$$

as exemplified in Fig. 16. For simplicity, we treat here the case of the initial lattice Λ belonging to the square system.

C1. Pure shear deformation

Here Λ' results from a pure shear deformation of the square lattice Λ of parameter $a = 1$ in the direction of angle α with the x axis of Λ and of intensity η :

$$\hat{\mathbf{a}} = \begin{pmatrix} 1 - \eta \cos \alpha \sin \alpha & \eta \cos^2 \alpha \\ -\eta \sin^2 \alpha & 1 + \eta \cos \alpha \sin \alpha \end{pmatrix}$$

with the shear direction $V_1 = (\cos \alpha, \sin \alpha)$.

If we choose: (i) the angle α among those generating a coincidence lattice,

$$\alpha = 2 \arctan \frac{m}{n},$$

as discussed in the body of this article, using $\sigma = n^2 + m^2$, and

$$\sigma \cos \alpha = n^2 - m^2 \text{ and } \sigma \sin \alpha = 2nm;$$

(ii) the shear intensity η rational with respect to the square lattice parameter

$$\eta = p/q, \quad p, q \in \mathbb{N}^+;$$

then the transformation $\hat{\mathbf{a}}$ is written as a matrix with rational coefficients,

$$\hat{\mathbf{a}} = \frac{1}{q\sigma^2} \begin{bmatrix} q\sigma^2 - 2pnm(n^2 - m^2) & p(n^2 - m^2)^2 \\ -4pn^2m^2 & q\sigma^2 + 2pnm(n^2 - m^2) \end{bmatrix},$$

which generates a coincidence lattice defined by the unit vectors

$$A = \frac{1}{\gamma}(n^2 - m^2, 2nm), \quad B = \frac{q}{\gamma}(-2nm, n^2 - m^2),$$

where $\gamma = \text{gcd}(n^2 - m^2, 2nm)$.

C2. 1D dilatation

A dilatation of the square lattice Λ of intensity ζ in the direction of angle α with respect to the x axis of Λ can be written as

$$\hat{\mathbf{a}} = \begin{pmatrix} 1 + \zeta \cos^2 \alpha & \zeta \cos \alpha \sin \alpha \\ \zeta \cos \alpha \sin \alpha & 1 + \zeta \sin^2 \alpha \end{pmatrix}.$$

As in the previous case, if $\zeta = p/q, p, q \in \mathbb{N}^+$ and $\alpha = 2 \arctan(m/n)$, the transformation $\hat{\mathbf{a}}$ is a matrix with rational coefficient

$$\hat{\mathbf{a}} = \frac{1}{q\sigma^2} \begin{bmatrix} q\sigma^2 + p(n^2 - m^2)^2 & 2pnm(n^2 - m^2) \\ 2pnm(n^2 - m^2) & q\sigma^2 + 4pn^2m^2 \end{bmatrix}$$

with lattice parameters

$$A = \frac{q+1}{\gamma}(n^2 - m^2, 2nm), \quad B = \frac{1}{\gamma}(2nm, m^2 - n^2)$$

where $\gamma = \text{gcd}(n^2 - m^2, 2nm)$.

Acknowledgements

Special thanks are due to Guy Trambly de Laissardière, Vincent Renard, Florie Mesple, Hakim Amara, Bertrand Toudic, Sylvie Lartigues-Korinek and Olivier Hardouin Duparc for very helpful discussions during the writing of the present paper. The very impressive and careful proofreading by one of the referees and their many suggestions were essential for improving the quality of the paper.

Funding information

Funding for this research was provided by: Agence Nationale de la Recherche (project ANR FLATMOI 21-CE30-0029-04G).

References

- Baake, M. & Grimm, U. (2006). *Z. Kristallogr.* **221**, 571–581.
- Baake, M. & Zeiner, P. (2017). *Aperiodic Order*, Vol. 2, *Crystallography and Almost Periodicity*, edited by M. Baake & U. Grimm, pp. 73–172. Cambridge University Press.
- Bistritzer, R. & MacDonald, A. H. (2011). *Proc. Natl Acad. Sci. USA*, **108**, 12233–12237.
- Campanera, J. M., Savini, G., Suarez-Martinez, I. & Heggge, M. I. (2007). *Phys. Rev. B*, **75**, 235449–235462.
- Cao, Y., Fatemi, V., Demir, A., Fang, S., Tomarken, S. L., Luo, J. Y., Sanchez-Yamagishi, J. D., Watanabe, K., Taniguchi, T., Kaxiras, E., Ashoori, R. C. & Jarillo-Herrero, P. (2018). *Nature*, **556**, 80–84.
- Cao, Y., Fatemi, V., Fang, S., Watanabe, K., Taniguchi, T., Kaxiras, E. & Jarillo-Herrero, P. (2018). *Nature*, **556**, 43–50.
- Coxeter, H. S. M. (1963). *Regular Polytopes*, 2nd ed. New York: Macmillan.
- Feuerbacher, M. (2021). *Acta Cryst.* **A77**, 460–471.
- Geim, A. K. (2009). *Science*, **324**, 1530–1534.
- Gratias, D. & Portier, R. (1982). *J. Phys. Colloq.* **43**, C6-15–C6-24.
- Gratias, D. & Quiquandon, M. (2020). *Crystals MDPI*, **10**, 560–574.
- Grimmer, H. (1973). *Scr. Metall.* **7**, 1295–1300.
- Grimmer, H. (1974). *Scr. Metall.* **8**, 1221–1223.
- Grimmer, H. (1984). *Acta Cryst.* **A40**, 108–112.
- Hahn, T. (2005). Editor. *International Tables for Crystallography*, Vol. A, *Space-Group Symmetry*, 5th ed. Heidelberg: Springer.
- Halphn, G. (1877). *Bull. Soc. Math. Fr.* **5**, 170–175.
- Hardy, G. H. & Wright, E. M. (1979). *An Introduction to the Theory of Numbers*, 5th ed. Oxford University Press.
- Hass, J., Varchon, F., Millán-Otoya, J. E., Sprinkle, M., Sharma, N., de Heer, W. A., Berger, C., First, P. N., Magaud, L. & Conrad, E. H. (2008). *Phys. Rev. Lett.* **100**, 125504–125508.
- Naik, M. H. & Jain, M. (2018). *Phys. Rev. Lett.* **121**, 266401–266407.
- Philippon, P. (2008). *Un œil et Farey*, <https://hal.science/hal-00488471>.
- Pleasant, P. A. B., Baake, M. & Roth, J. (1996). *J. Math. Phys.* **37**, 1029–1058.
- Pond, R. C. & Vlachavas, D. S. (1983). *Proc. R. Soc. Lond. Ser. A*, **386**, 95–143.
- Ranganathan, S. (1966). *Acta Cryst.* **21**, 197–199.
- Romeu, D., Aragón, J. L., Aragón-González, G., Rodríguez-Andrade, M. A. & Gómez, A. (2012). *Cryst. Struct. Theory Appl.* **01**, 52–56.
- Soriano, D. & Lado, J. L. (2020). *J. Phys. D Appl. Phys.* **53**, 474001–474012.
- Suárez Morell, E., Correa, J. D., Vargas, P., Pacheco, M. & Barticevic, Z. (2010). *Phys. Rev. B*, **82**, 121407–121411.
- Trambly de Laissardière, G., Mayou, D. & Magaud, L. (2010). *Nano Lett.* **10**, 804–808.
- Trambly de Laissardière, G., Mayou, D. & Magaud, L. (2012). *Phys. Rev. B*, **86**, 125413–125420.
- Varchon, F., Mallet, P., Magaud, L. & Veuillen, J.-Y. (2008). *Phys. Rev. B*, **77**, 165415–165420.
- Venkateswarlu, S., Honecker, A. & Trambly de Laissardière, G. (2020). *Phys. Rev. B*, **102**, 081103–081109.
- Wu, F., Lovorn, T., Tutuc, E., Martin, I. & MacDonald, A. H. (2019). *Phys. Rev. Lett.* **122**, 086402–086407.